Presentations and Additional Papers

TESTING OF THE PROPOSED IERS 2000 CONVENTION SUB-DAILY EARTH ROTATION PARAMETER MODEL

J. Kouba
Natural Resources Canada, Geodetic Survey Division,
615 Booth Street, Ottawa, Canada K1A 0E9
email: kouba@geod.nrcan.gc.ca

Abstract

The differences between the proposed International Earth Rotation Service (IERS) 2000 and the conventional IERS 1996 sub-daily Earth rotation parameters (ERP) models can reach 0.1 mas and 0.1 mas/day. The largest differences are seen for the beat periods of 14.2 and 360 days, which correspond to the diurnal tidal waves of O1 and (K1, P1), respectively. Precise independent polar motion (PM) rate solutions effectively doubles the sampling rate and allows for effective testing of sub-daily ERP models and other periodical effects at the diurnal and semi-diurnal frequency bands. The JPL independent daily PM rate solutions, which on November 12, 2000 have switched to the conventional IERS 1996 sub-daily ERP model from the older model of Herring and Dog (1994), show no or greatly reduced 14.2 day amplitude (O1) peaks. This confirmed that the anomalistic amplitudes at 14.2 day period seen for JPL PM solutions prior November 12, 2000 was largely due to the use of the older sub-daily ERP model. The new IERS 2000 sub-daily ERP model is expected to perform equally well, or slightly better than the conventional IERS 1996 model, as indicated by the JPL PM rate solutions, which were corrected for the IERS 1996 and 2000 model differences.

1. Introduction

Since June 30, 1996 the International GPS Service (IGS) has adopted the sub-daily ERP model (for PM and UI1-UTC), based on the International Earth Rotation Service (IERS) 1996 Conventions, in all IGS Analysis Center (AC) analyses (Neilan et al., 1996). All ACs have complied and have been using sub-daily ERP models. However, early in 1999, while analyzing IGS and AC ERP rate solutions with respect to Atmospheric Angular Moment (AAM) data, a significant anomalistic, 14.2-day period spectral peaks were noted for the Jet Propulsion Laboratory (JPL) ERP solutions (Kouba et al., 2000). Latter on this was confirmed to be due to a different sub-daily ERP model (*Herring and Dong, 1994)*, used by JPL up to MJD 51860 (November 12, 2000) (Kouba, 2002).

Table 1: Differences between *Herring and Dong (1994)* and the conventional *IERS (1996)* sub-daily ERP models for X_P, Y_P pole positions. The beat periods are the periods with which the tidal waves beat against the period of exactly 24-h UTC. (*Herring and Dong (1994)–IERS (1996)*); prograde (+), retrograde(-))

Tide wave	Period(h)	Beat Per.(d)	X_P cos(mas)	X_P sin(mas)	Y_P cos(mas)	Y_P sin(mas)
M2	12.42	14.75	0.0370	-0.0070	0.0117	0.0253
S2	12.00	∞	0.0002	-0.0345	-0.0004	-0.0098
N2	12.66	9.62	0.0107	0.0018	0.0018	-0.0103
K2	11.97	-181.32	-0.0296	-0.0152	-0.0102	-0.0473
K1	23.94	-368.23	0.0190	-0.0042	0.0042	0.0190
O1	25.82	14.19	0.0449	-0.0404	0.0404	0.0449
P1	24.07	364.64	-0.0013	-0.0099	0.0099	-0.0013
Q1	26.87	9.37	0.0068	-0.0047	0.0047	0.0068

For completeness, the current conventional sub-daily ERP model *IERS (1996)* and the older *Herring and Dong (1994)* model are compared in Table 1, taken from Kouba (2002). The differences of Table 1 indicate that the 14.2 and 180 day (beat period) anomalies noticed in 1999 are mainly due to the use of the older sub-daily ERP model. This is so, since the tidal waves O1 and K2, which have the beat periods (against exactly 24h UTC) of 14.2 and 181.3 days, also show the largest differences. An analysis of the most recent

JPL PM solutions (after Nov. 12, 2000), which are based on the IERS (1996) conventions, confirmed this, since the apparent 14.2 day amplitudes for X_P and Y_P were significantly decreased *(Kouba, 2002)*. This demonstrates not only the sensitivity of independent ERP rate solutions to the sub-daily ERP effects, but also the capability to detect possible sub-daily ERP model deficiencies while using the existing *ERP* rate solutions with the standard sampling rate of 24-h.

2. IERS 1996 and IERS 2000 sub-daily ERP model differences

IERS is about to adopt a new set of conventions (IERS, 2000) which include a new sub-daily ERP model, which is still supposed to be consistent with the IERS (1996) model, i.e. it is also based on the model of Ray et al., (1994). However, the proposed IERS (2000) model has been extended by a number small tidal waves derived by a standard admittance from a recent ocean tide model, so that it now includes 71, rather than the eight principal tidal waves of IERS (1996) listed in Table 1. The pertinent question now is how much better the new sub-daily ERP model performs and whether it is worthwhile for IGS to switch to this new conventional ERP model. The IERS 1996 and IERS 2000 sub-daily ERP model differences for the period of the current IGS ERP series are plotted Figures 1a-c. For comparison purposes the complete sub-daily ERP signal based on the IERS 2000 model is also shown in each figure. In order to quantify the effect of the sub-daily ERP on independent ERP rate solutions, both the IERS 2000 pole position corrections and the corresponding differences between the IERS2000 and IERS1996 models have been fitted for apparent 24-h ERP rates. The apparent 24-h pole motion (PM) X_p and Y_p rates are shown in Figures 2 a-b. The spectra corresponding to Figures 1 and 2 are shown in Figure 3 and 4, respectively.

The model difference shown in Figures 1a-c are fairly large, when considering that both models are supposed to be based on the same model of Ray et al. (1994). Although the model differences are exceeding the formal precision of IGS ERP solutions (< 0.1 mas), they do not affect the ERP solutions as they are largely averaged out over the 24-h interval sampling used for all IGS ERP solutions. (This may not be the case for other solution parameters, such as precise orbits). However, the apparent rate differences, shown in Figures 2 a-b, may be significant and should be a matter of concern, as they map directly into independent ERP rate solutions and since they are also approaching the solution precision level of 0.1 – 0.2 mas/day. In particular, the 14- and 360-day periods seem to be predominant for the model differences as seen in Figure 4.

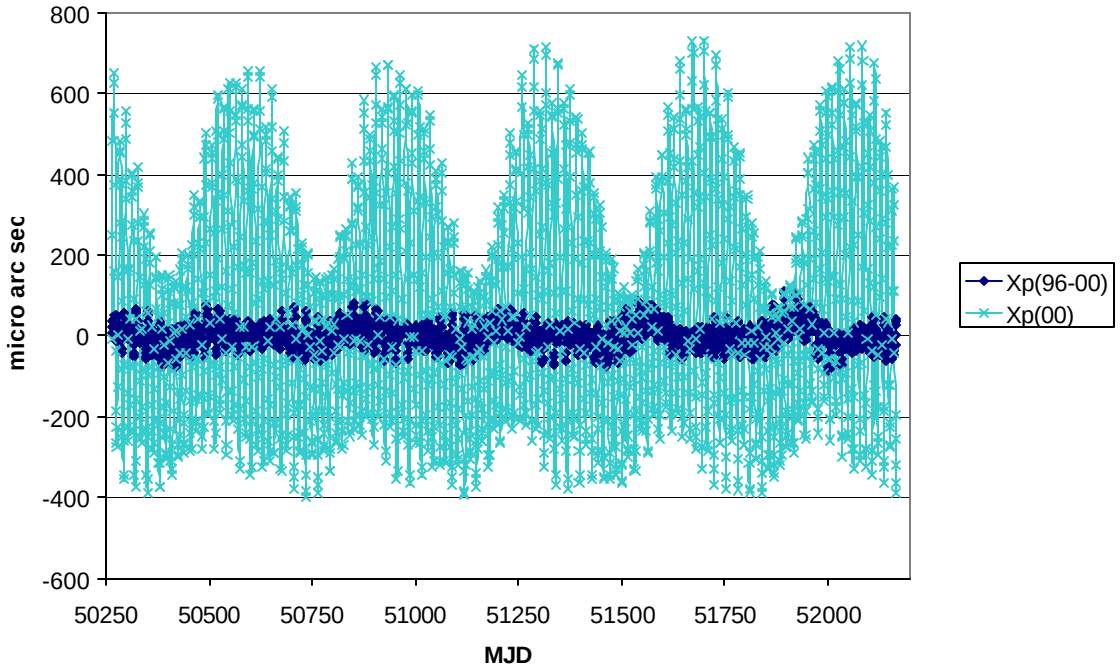

Figure 1a : IERS 1996 (96) and IERS 2000 (00) conventional ERP model differences for PM X_P.

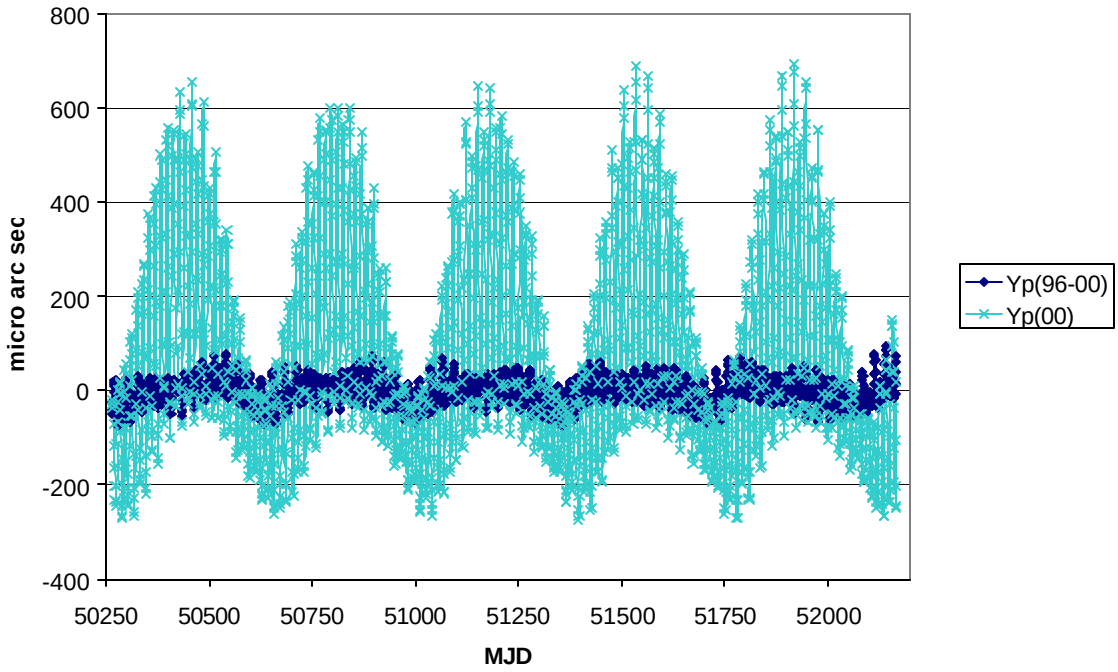

Figure 1b: IERS 1996 (96) and IERS 2000 (00) conventional ERP model differences for PM Y_P.

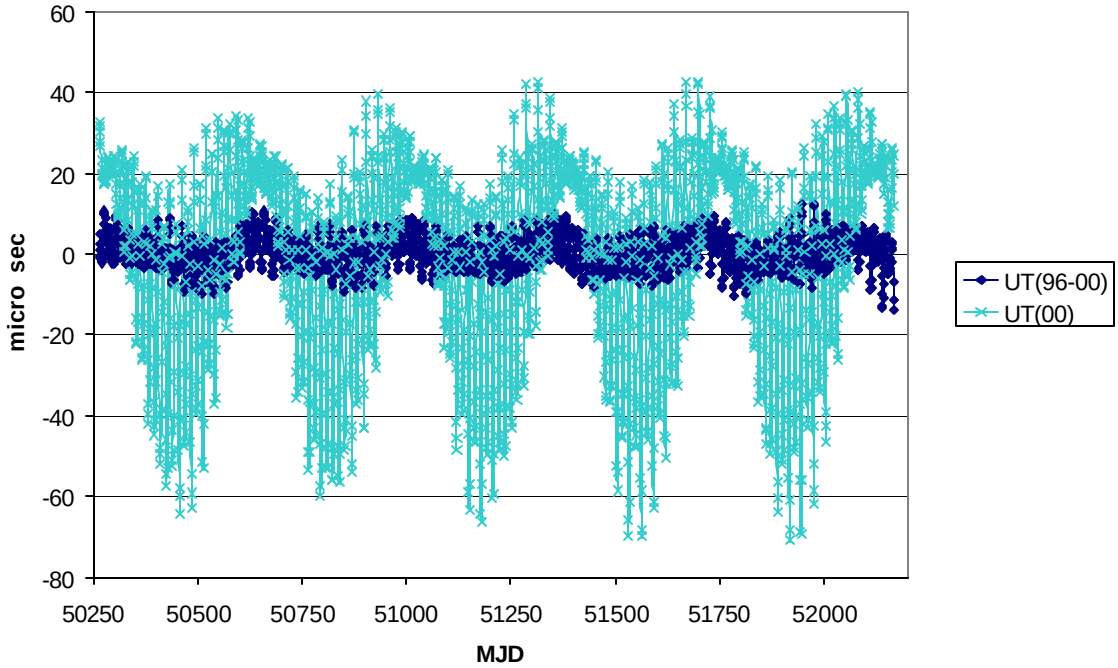

Figure 1c : IERS 1996 (96) and IERS 2000 (00) conventional ERP model differences for UT1-UTC (UT).

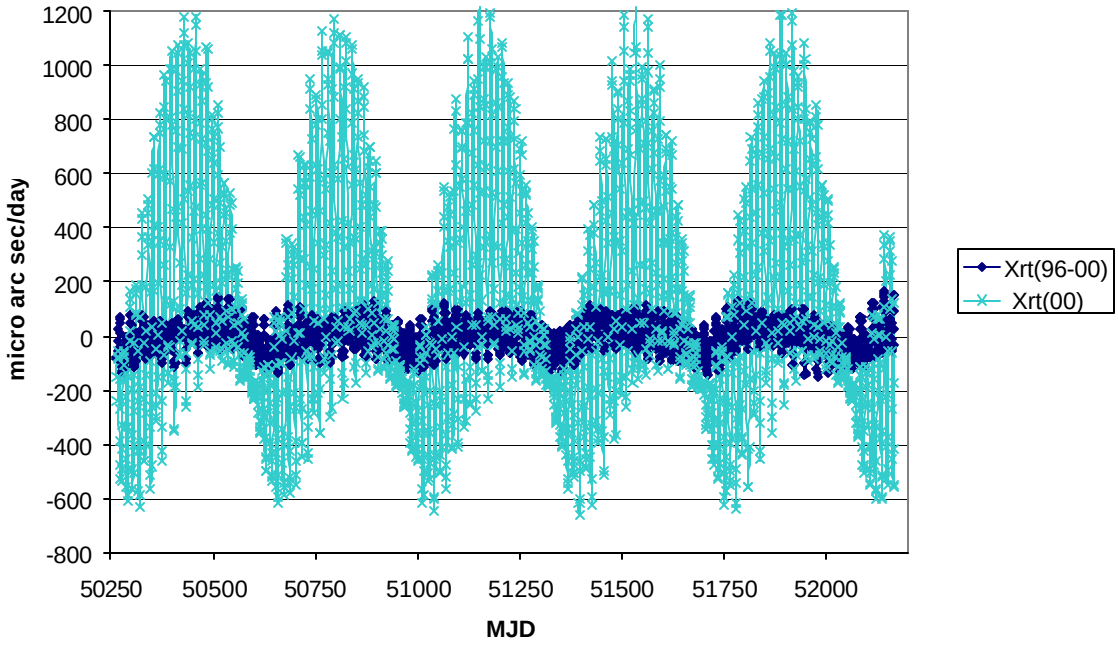

Figure 2a: Apparent PM X_P rate differences of IERS 1996 (96) and IERS 2000 (00) conventional models.

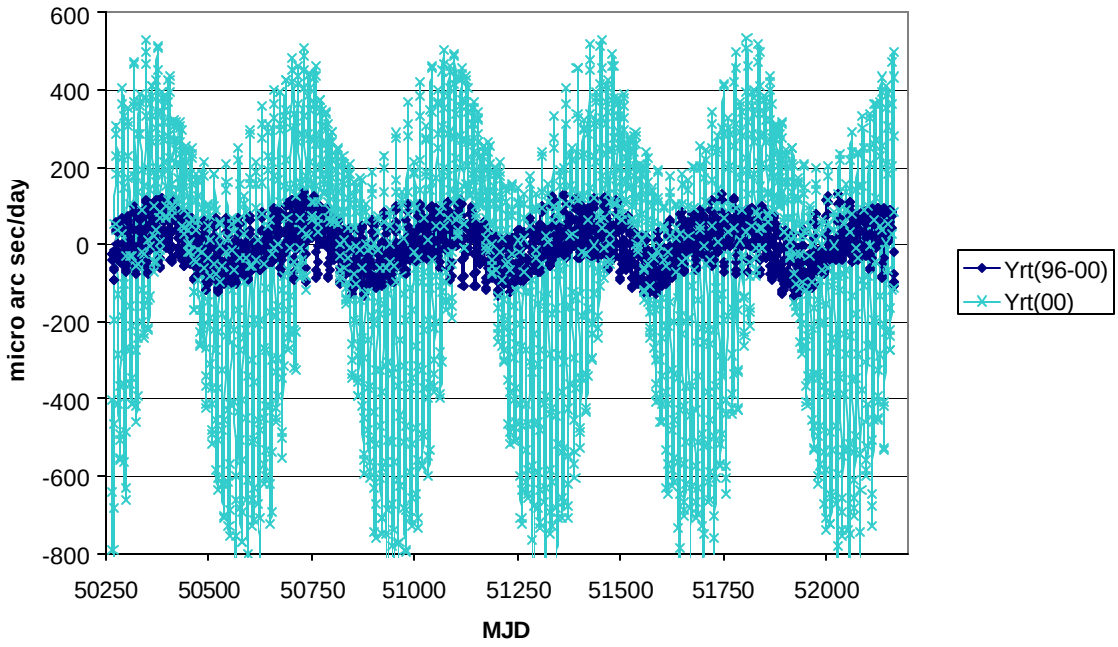

Figure 2b: Apparent PM Y_P rate differences of IERS 1996 (96) and IERS 2000 (00) conventional models.

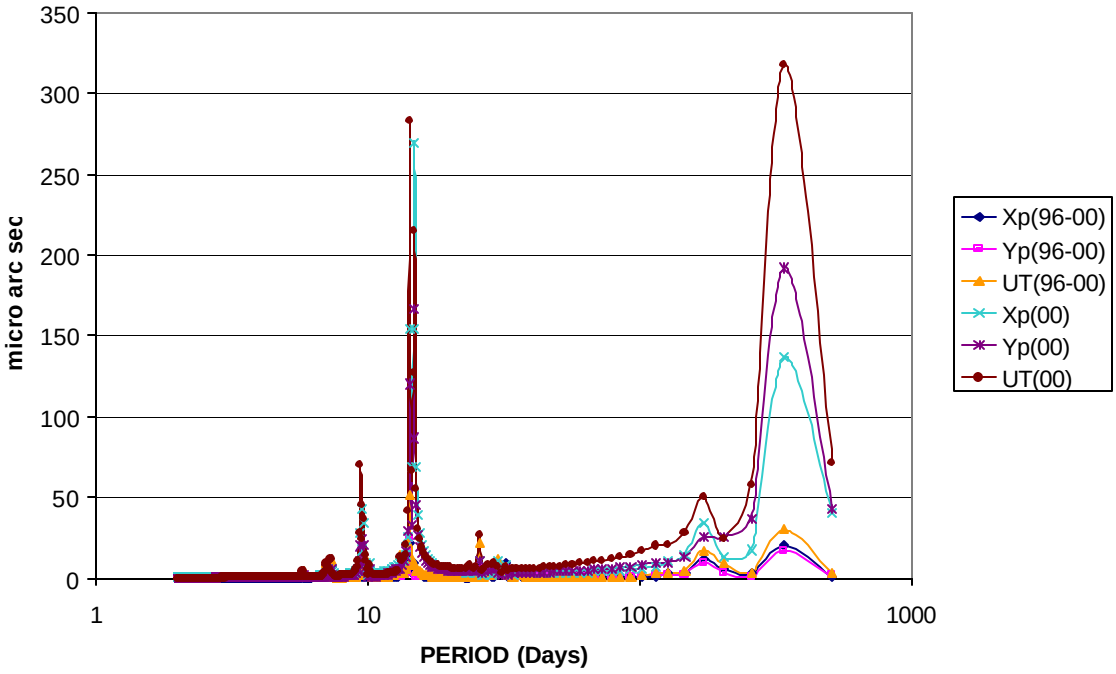

Figure 3: Spectra of IERS 1996 (96) and IERS 2000 (00) conventional ERP model differences.

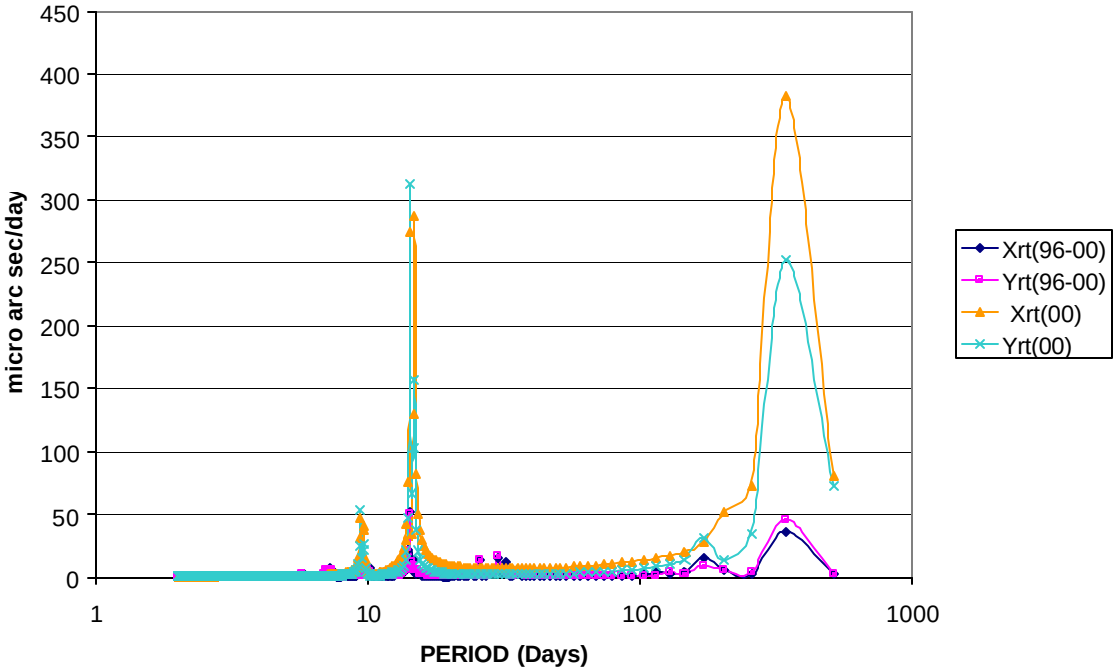

Figure 4: Spectra of apparent PM rate differences of IERS 1996 (96) and IERS 2000 (00) conventional models.

3. Testing methodology

To test a sub-daily ERP model, it is necessary either to solve for ERP at intervals much shorter than the current IGS sampling of 24-h, or solving it directly by including significant diurnal and semidiurnal tidal terms amongst the solution parameters. In both cases, the retrograde (negative) diurnal polar motion (PM) signal must be suppressed, as in GPS global analyses it is completely correlated with the orientation of the solved GPS satellite orbits (*Rothacher 1998; Rothacher at al., 2001).* However, both of these approaches require specialized processing and cannot take the advantage of the wealth of the existing, long and precise AC solutions as well as the IGS combined product series. . An alternative approach used here is to analyze the existing series of long and precise AC and IGS ERP and ERP rate solutions with 24-h sampling and to examine the beat periods that are listed in the third column of Table 1. The independent 24-h ERP rate solutions are quite sensitive to the signals at the diurnal and semi-diurnal tidal frequency bands (see Figures 2a, b and e.g., Kouba, 2002). However, continuity constraints applied by most ACs and in the currently official IGS Final ERP series (IGS00P02), completely suppress any such signals at the diurnal and semi-diurnal tidal frequency bands. Kouba et al. (2000) have successfully used the ERP rates derived from Atmospheric Angular Momentum (AAM) data to detect the JPL anomalistic periods at 14.2 and 181 days which were caused by using a sub-daily ERP model that did not conform to the IERS (1996) conventions. This kind of comparisons revealed the above beat periods as well as other, long period ERP rate signals that were not contained in the AAM and which correlated with oceanic and even ionospheric effects (Kouba et al., 2000)

For the tests here, a different comparison was used which was specifically designed to detect only the beat periodical signals at diurnal and sub-diurnal frequencies. Such signals can be real (e.g. due to the oceans, atmosphere), or only apparent (e.g. due to (orbit) modeling deficiencies). Since the UT rate, i.e. the length of day (LOD) is subjected to a number of zonal tidal terms, some of which have the same periods as the expected beat periods of the sub-daily ERP effects, here only PM rate solutions were used in this testing. More specifically, the following daily PM rate differences (dX) can be used for this purpose:

$$dX(t_{i+0.5}) = X(t_{i+1}) - X(t_i) - [Xrt(t_{i+1}) + Xrt(t_i)]/2, \qquad (1)$$

where $X(t_{i+1})$, $X(t_i)$ and $Xrt(t_{i+1})$, $Xrt(t_i)$ are the pole position and pole rate solutions at the two adjacent daily epochs t_{i+1} and t_i , respectively. The quantity (1) can be interpreted as either the pole position difference at the mid points, interpolated either from the subsequent or preceding pole position with the pole rate solutions. Alternatively, it can also be interpreted as the difference between the pole rates derived from the solved pole positions and the pole rate solutions. Since the 24-h average pole position solutions, unlike the independent 24-h pole rate solutions, are insensitive to any diurnal and semi-diurnal signals, the rate difference (1) will fully reflect the real (e.g. due to ocean/atmosphere) and apparent (e.g. orbit model errors) signals, but only at the beat frequencies of the diurnal/semi-diurnal tidal bands. The other, long period signals, will cancel out in (1), since they are contained in both the pole position and pole rate solutions. Note that the expression (1) is quite suitable for a detection of the (beat) periods that are much longer than two days, since the random noise of the rate solutions is reduced by $\sqrt{2}$ (due to the averaging over the two adjacent days). Yet the long period signals (>> 2 days) are not affected by this averaging. Furthermore, the error contributions of the pole position difference in (1) is relatively small, since the 24-h average pole position solutions are more precise, by at least a factor of 2, than the corresponding rate solutions. Subsequently, the error contribution of the pole position difference in (1) is typically smaller than the averaged rate solution errors in (1). Expression (1) also demonstrates that by solving for independent pole rate, the sampling rate of pole rate series effectively doubles, i.e. the observed pole rate series and the one computed from the corresponding pole position solutions are offset by 0.5 day in this case. However, when the ERP continuity constraints are enforced in the pole rate solutions, both the computed and observed pole rate series become equivalent and the rate differences of (1) becomes equal to zero, and cannot be used for such sub-daily ERP tests. This can be seen in Figure 5, which shows a recent segment of the rate differences (1), evaluated from the new IGS Final ERP combined series (IGS00P02) which clearly contains continuity constraints during each week.

The ERP rate continuity within each week of the IGS00P02 series is the consequence of unremoved/unreported continuity constraints in at least one of the submitted AC weekly SINEX solutions. Since, as long as even a single AC SINEX solution contains the unremoved ERP continuity constraints within its weekly SINEX variance-covariance matrix, then the rigorously combined IGS SINEX solutions (which includes the corresponding variance-covariance matrices) for IGS00P02.erp will also include the ERP rate continuity constraints within the current week. There is no ERP continuity between subsequent weeks, as the AC weekly SINEX submissions are considered independent from week to week within the IGS SINEX combinations. Thus the weekly ERP rate discrepancies are clearly visible in Figure 5.

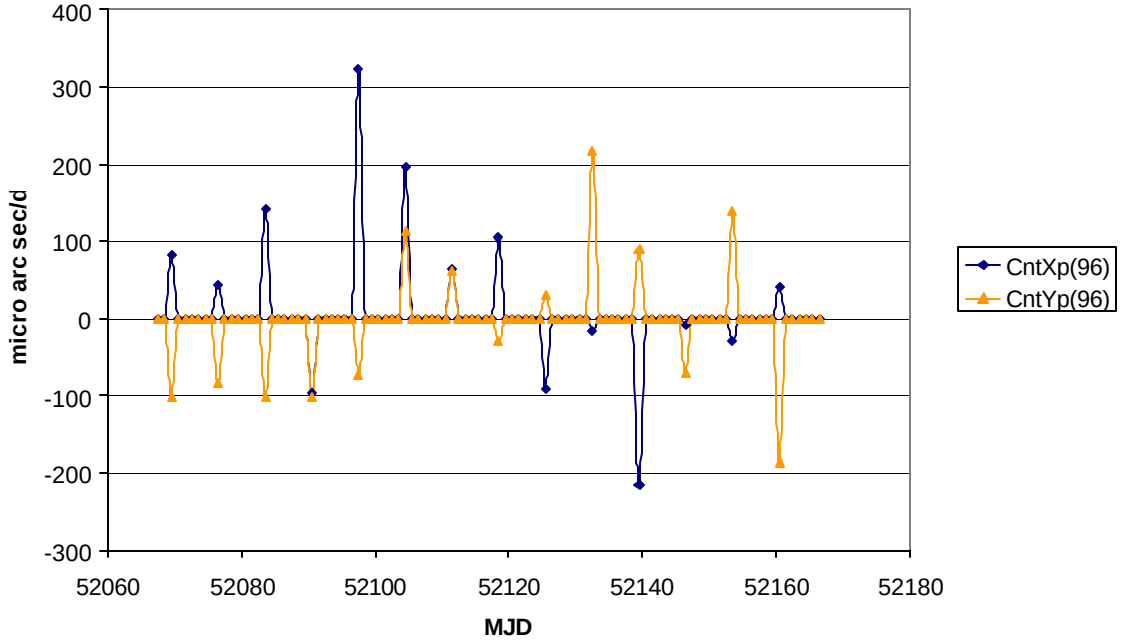

Figure 5: Pole rate differences (1) for the IGS Final ERP combination series (IGS00P02.erp).

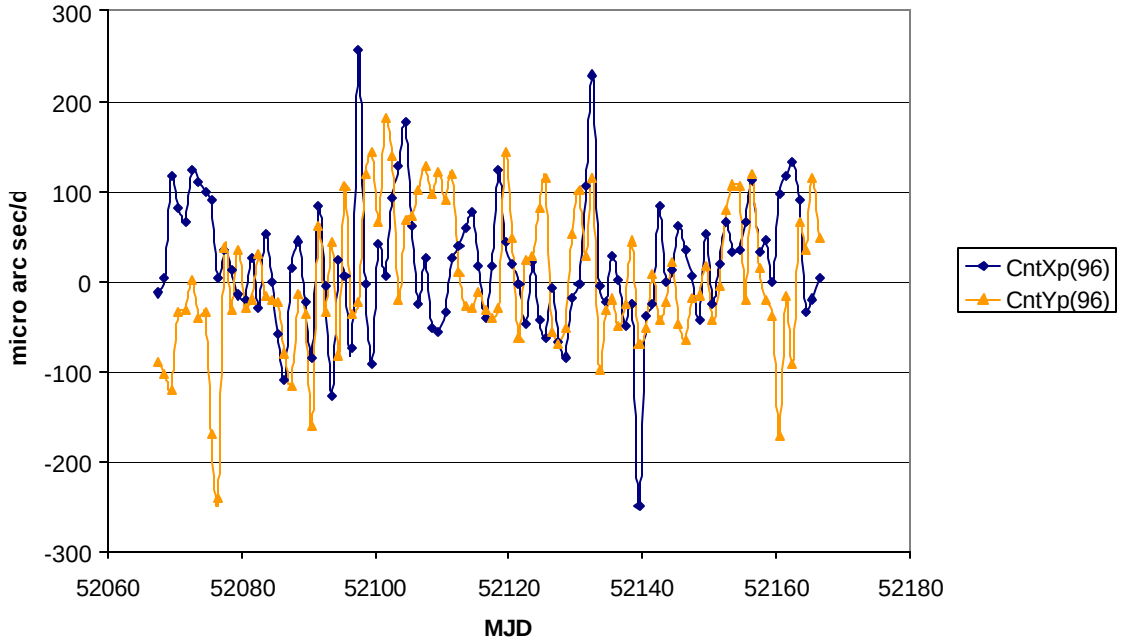

Figure 6: Pole rate differences (1) for the original IGS Final ERP Combination series (IGS95P02.erp)

Unfortunately, most ACs have chosen to apply the continuity constraints in their ERP rate solutions, so that the rate differences (1) are largely suppressed also in the original, independently combined, IGS ERP series (IGS95P02). This original IGS combined series, which was superceded by the SINEX combination (IGS00P02) in early 2000, is generated independently within the orbit/clock Final combinations, while also utilizing for the ERP combinations the objectively determined, orbit weights (Beutler et al., 1995). The IGS95P02 differences are shown in Figure 6. Since only two ACs (JPL and EMR) are confirmed to solve for independent ERP rates (Kouba et al., 2000), then the IGS95P02 signal of (1) is expected to be attenuated by a factor of about 0.25, which should correspond to an average proportional combined weight of the two AC solutions within the orbit/ERP combination process (*Mireault, 2001, person. Comm.*). Furthermore, as already noticed, prior MJD 51860, the JPL AC solutions, which up to November 12, 2000 were based on a different sub-daily ERP model, are also included within the IGS95P02 series.

4. Results

Since only JPL and EMR ACs are known to submit independent ERP rate solutions, they were chosen for the testing. For the sake of completeness, both IGS Final ERP series were also used, i.e. the original independently combined IGS Final ERP series (IGS95P02.erp), which reflects only partly any discontinuities of (1), as well as the official IGS Final ERP (IGS00P02.erp), which is combined rigorously within SINEX station/ERP combinations, and which appears to have continuity constraints (see Figure 5). Furthermore, since JPL has used the Herring and Dong (1994) sub-daily ERP model prior November 12, 2000 (MJD 51860), the JPL solutions were subdivided into two equal sets of 8.5 month, one before and one after the model change. For the second set, which is based on the IERS (1996) model, the corresponding ERP solutions also have been obtained with the proposed IERS (2000) model. This was accomplished by simply adding the IERS 1996-IERS 2000 apparent (X_P, Y_P) rate differences (see Figures 2a, b) to the JPL ERP rate solutions based on the IERS (1996) sub-daily ERP model. This should be a legitimate approximation of an actual processing with the new IERS (2000) model, since the apparent rates caused by the sub-daily ERP effects are expected to map directly into the independent ERP rate solutions.

The resulting periods and amplitudes for the JPL PM (prograde and retrograde) rate solutions are shown in Figure 7 and 8. One can readily notice the significant improvements after the change from the Herring and Dong (1994) to the IERS (1996) model. This is true in particular for the noted 14.2-day period for which the retrograde amplitude of about 160 μarcsec practically vanished. This is quite consistent with the Table 1, which shows the largest differences for the tidal wave O1 with the beat period of 14.19 days. Furthermore, most amplitudes for longer periods, in particular for retrograde rotation (Figure 8), are smaller for the IERS (1996) model than for the Herring and Dong (1994) one. The IERS (2000) model, for most periods, gives the same or slightly smaller amplitudes for the recent JPL solutions, as can be observed in both Figures 7 and 8.

Note that the spectra of the IERS (2000)-IERS (1996) pole rate differences, abbreviated (00-96), are also shown in Figure 7 and 8 for a reference. A more complete spectra of the IERS (2000)-IERS (1996) pole rate differences, based on the whole period of Figures 1 and 2, were already shown in Figure 4. Note that for the two 8.5 month solution intervals of Figures 7 and 8, it is not yet possible to get any meaningful results for periods which are longer than 4 months, including the seasonal and semi-seasonal terms.

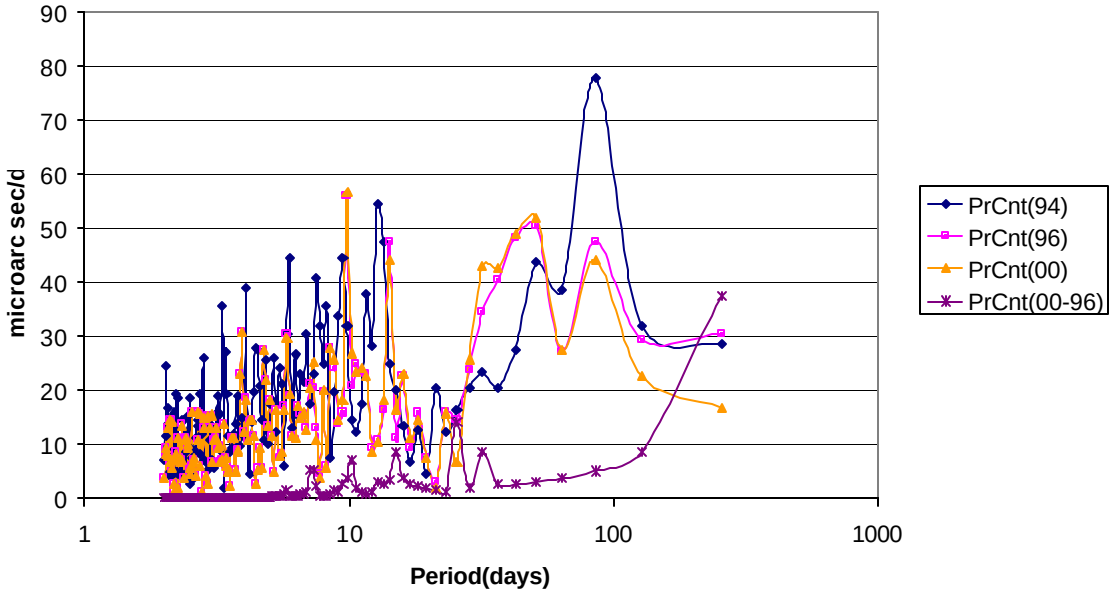

Figure 7: Spectra of JPL prograde PM rate discontinuities (1) for February 2000 to July 2001. (Sub-daily ERP models: Herring and Dong 1994 (94) used prior November 12, 2000; IERS 1996 (96) and IERS 2000 after November 12, 2000)

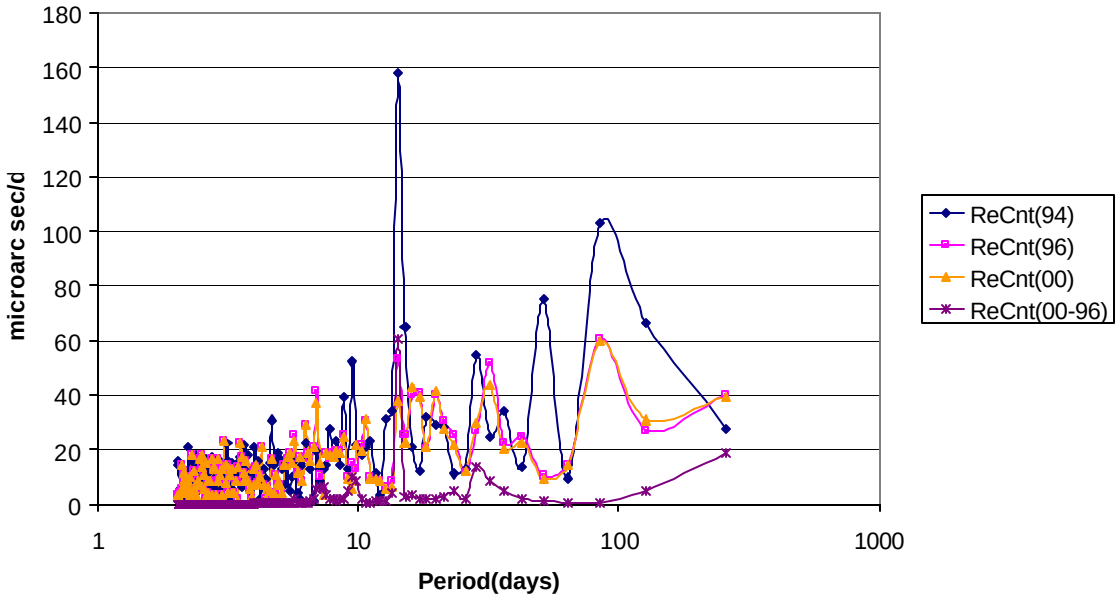

Figure 8: Spectra of JPL retrograde PM rate discontinuities (1) for February 2000 to July 2001. (Sub-daily ERP models: Herring and Dong 1994 (94) used prior November 12, 2000; IERS 1996 (96) and IERS 2000 (00) after November 12, 2000)

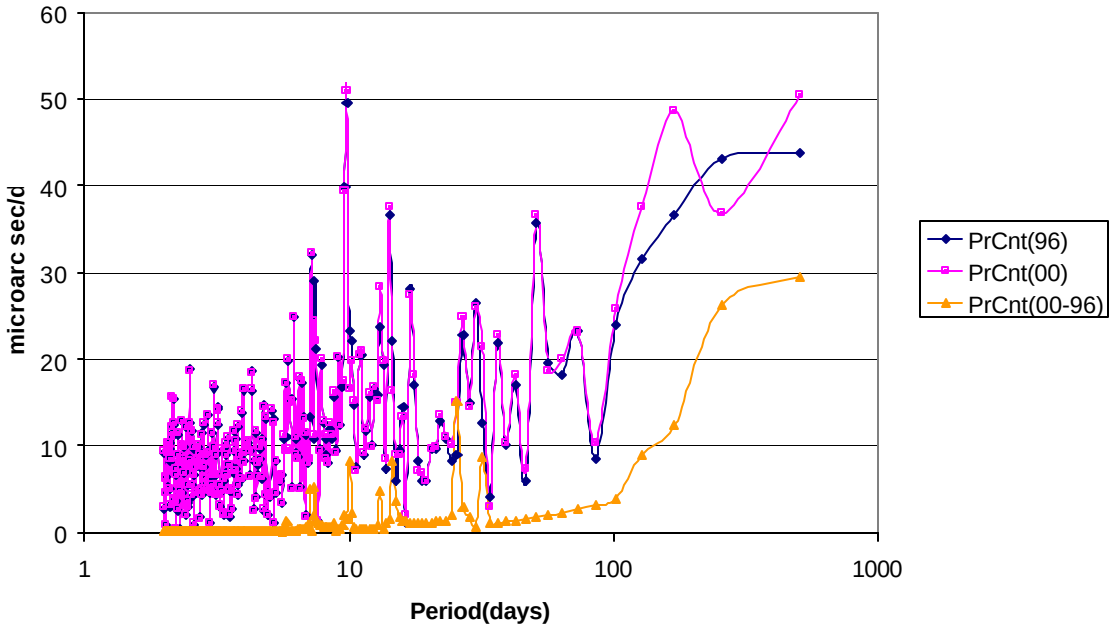

Figure 9: Spectra of EMR prograde PM rate discontinuities (1) for April 2000 to September 2001. (Sub-daily ERP Models: IERS 1996 (96) and IERS 2000 (00))

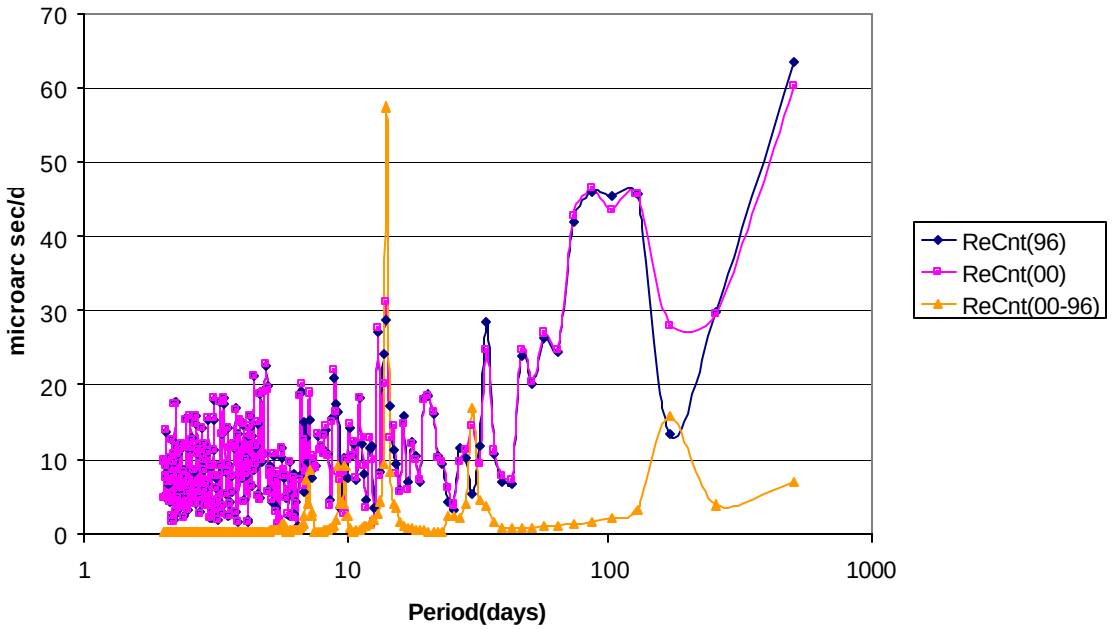

Figure 10: Spectra of EMR retrograde PM rate discontinuities (1) for April 2000 to September 2001. (Sub-daily ERP models: IERS 1996 (96) and IERS 2000 (00))

For the EMR solutions, a different interval, covering about 17 months of the most recent EMR ERP solutions, was used. During this period the EMR solutions should be fairly homogenous and are based only on the IERS (1996) model. Similarly as above, the IERS (2000) EMR solutions were simulated by adding the corresponding IERS (1996)-IERS (2000) apparent rate difference of Figure 2. The results are shown in Figures 9 and 10. Unlike for JPL, the EMR results based on the IERS (2000) model did not seem to improve with respect to the IERS (1996) model results. This may be due to the fact that EMR ERP rate

solutions are considerably noisier (by a factor of about 2) than the JPL PM rate solutions and thus may be affected by larger solution biases. In particular, the large amplitude in seasonal and semi-seasonal bands are disturbing and should be investigated by using solution intervals much longer than 17 months used here.

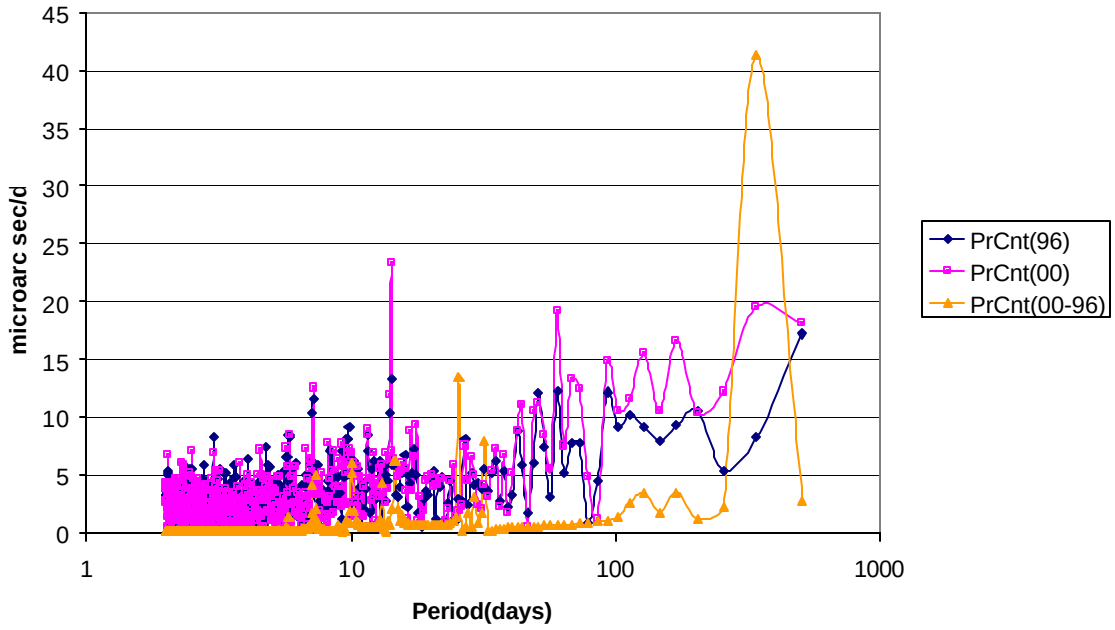

Figure 11: Spectra of IGS95P02 prograde PM rate discontinuities (1) for Nov. 1998 to September 2001. (Sub-daily ERP models: IERS 1996 (96) and IERS 2000 (00); PrCnt(00)=PrCnt(96)-0.25 PrCnt(00-96))

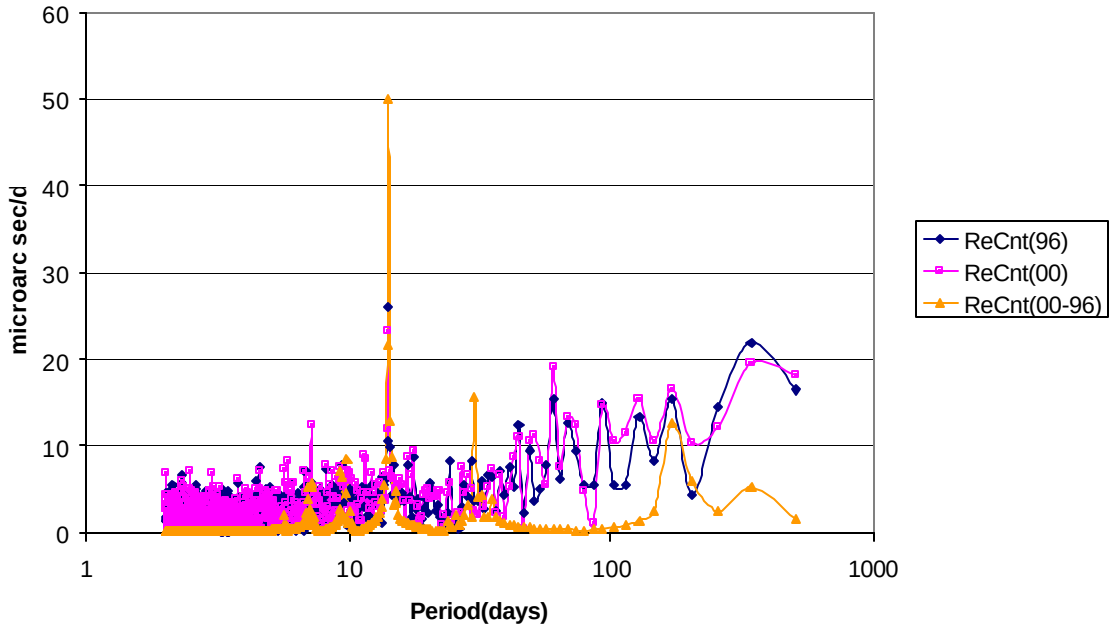

Figure 12: Spectra of IGS95P02 retrograde PM rate discontinuities (1) for Nov. 1998 to Sep. 2001. (Sub-daily ERP models: IERS 1996 (96) and IERS 2000 (00); ReCnt(00)=ReCnt(96)-0.24 ReCnt(00-96))

Figures 11 and 12 show results for the original, independently combined, IGS Final ERP series (IGS95P02) and for the entire observation period. Unlike for the JPL and EMR ERP series, the expected IERS (2000)

model results were generated by adding only 25% of the IERS (1996)-IERS (2000) model difference, also shown here. This reflects the expected proportional weighting of the two independent ERP rate solutions within the IGS orbit/ERP/clock combinations and the fact that the rest of ACs were employing continuity constraints during each week.

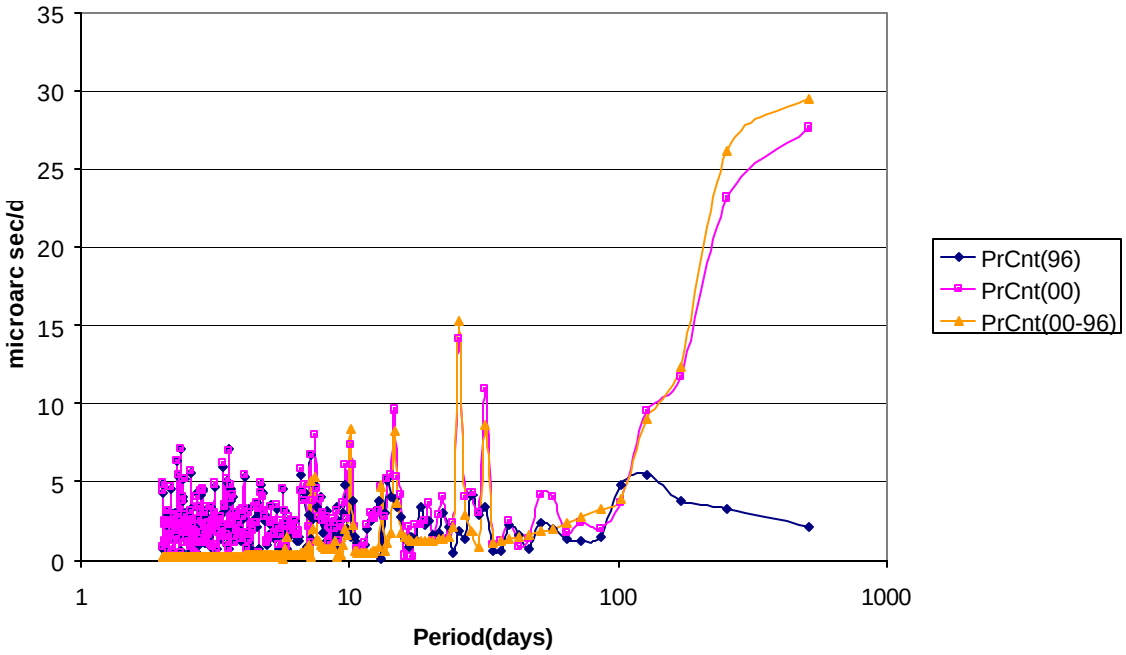

Figure 13: Spectra of IGS00P02 Prograde PM Rate Discontinuities (1) for April 2000 to September 2001. (Sub-daily ERP Models: IERS 1996 (96) and IERS 2000 (00); PrCnt(00)=PrCnt(96) - PrCnt(00-96))

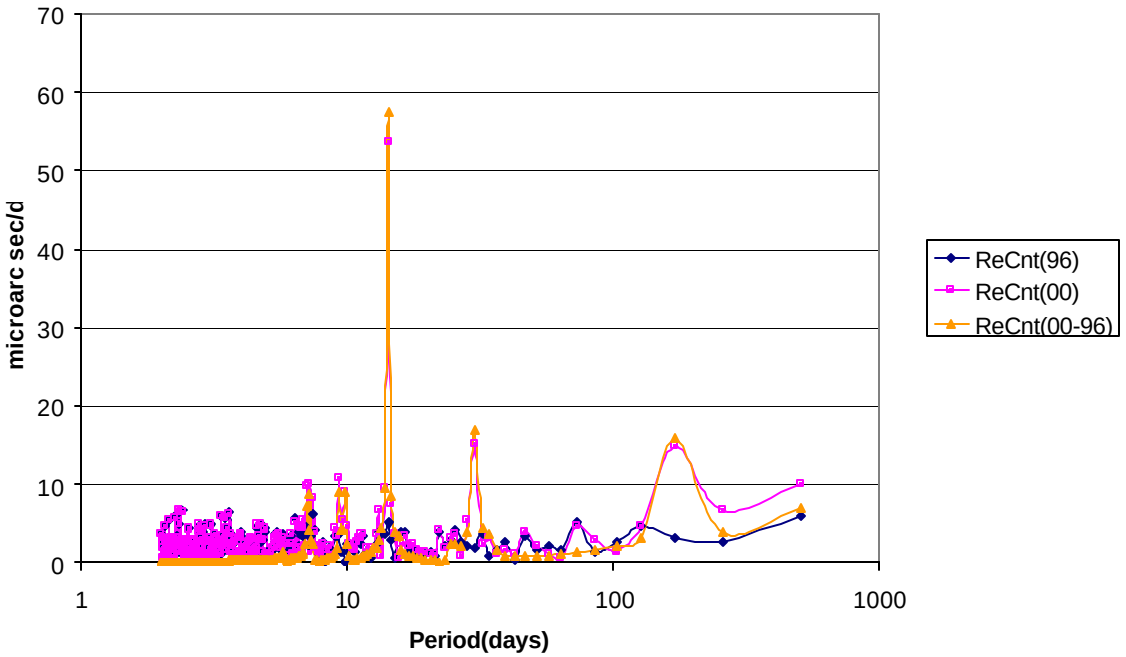

Figure 14: Spectra of IGS00P02 Retrograde PM Rate Discontinuities (1) for April 2000 to September 2001. (Sub-daily ERP Models: IERS 1996 (96) and IERS 2000 (00); ReCnt(00)=ReCnt(96) - ReCnt(00-96))

Further complications, which diminishes the significance and usefulness of the IGS95P02 results, is the fact that these combinations also include, with relatively high weights, the JPL ERP rate solutions prior Nov. 12, 2000. These JPL solutions, as already discussed and shown above, were based on an unconventional model of Herring and Dong (1994). Nevertheless, the IGS95P02 results based on the IERS 2000 model also seem to perform equally well with the IERS (2000) sub-daily ERP model. Although the seasonal differences shown in Figures 11 and the 14.2 peaks in Figure 12 are relatively large and somewhat disturbing. Note they are not consistent with the JPL results based on IERS (2000), shown in Figures 7 and 8, which had decreased amplitudes for prograde seasonal and retrograde 14.2-day amplitudes, respectively. However, the JPL seasonal and semi-seasonal amplitudes of Figure 7 and 8 should not be considered reliable, given the short solution intervals that were used for the JPL solutions. Note that Figures 11 and 12, for completeness, contain the sub-daily PM rate model difference spectra (00-96) for the entire period, and that they were already shown in Figure 4, but in a much smaller scale and for the X_P and Y_P components.

Figures 13 and 14, which show the official IGS ERP series (IGS00P02) that appears to include the ERP continuity constraints, are included only for completeness and to show how any apparent ERP rate signal is suppressed down, nearly to zero in this case. Consequently, the model IERS (2000) – IERS (1996) differences and the derived series based on IERS (2000), this time using 100% of the IERS 2000 - IERS 1996 difference, show much larger and practically the same amplitudes. This demonstrates the relative size of the model difference signal with respect to the continuity-imposed series discontinuities (1), which give practically zero amplitudes for all periods.

Table 2: Pole Rate RMS for Tested AC and IGS ERP Rate Solutions (in micro arc sec/day)

AC/IGS		Herring & Dong (1994)		IERS(1996)		IERS(2000)		IERS(1996-2000)	
		Xrt	Yrt	Xrt	Yrt	Xrt	Yrt	Xrt	Yrt
JPL	mean	-11	-69	6	-44	-2	-47	2	-5
	RMS	250	286	188	202	189	195	59	59
EMR	mean			-59	21	-66	18	2	-5
	RMS			246	276	250	277	59	59
IGS95	mean			0	3	0	4	2	-5
	RMS			78	95	76	95	59	59
IGS00	mean			4	-2	3	-1	2	-5
	RMS			43	52	45	54	59	59

The time domain statistics (means and RMS about the means) for the ERP solutions and intervals shown in Figures 7-14 are summarized in Table 2. As one can see, the conventional IERS (1996) performed significantly better than the older Herring and Dong (1994) model and the proposed new convention IERS (2000) performed equally well as the IERS (1996) sub-daily ERP model. Note that the derived IERS (2000) statistics for IGS95 (IGS95P02), like in Figures 11-12, used only 25% of the IERS (1996-2000) model difference, in order to approximate the relative weighting of AC solutions within the IGS ERP combinations (IGS95P02).

5. Conclusions

An efficient test of the sub-diurnal ERP effects was developed and successfully tested with precise independent ERP rate solutions. Such tests, involving the continuity conditions of ERP and ERP rate solutions, are non zero and meaningful only for independent ERP rate solutions. Furthermore, they are sensitive only to sub-diurnal effects caused e. g. by the oceans, atmosphere or solution model inadequacies, since the other, long period effects, are the same for both the ERP and ERP rate solutions, thus they completely cancel out. However, this continuity testing is not possible for the currently official IGS Final ERP series and the most of the AC ERP rate solutions, for which ERP rate continuities are enforced during each week.

The continuity tests, using the independent JPL ERP rate solutions, were able to confirm the differences between two sub-daily ERP models. The tests also indicated that the new IERS 2000 model is performing equally well or slightly better than the conventional model of IERS 1996. This is true in particular for the *O1* tidal frequency (i.e. at the corresponding 14.2-day beat period) and for JPL solutions. The analyses of a noisier EMR ERP solution series did not produce any such indication. In this case, an interval longer than the 17 months should be used, provided that the EMR solutions could be considered homogenous during such longer interval.

6. Acknowledgements

The International GPS Service is an unprecedented and voluntary, yet coordinated cooperation amongst many government and university agencies, and individuals, allowing efficient and precise use of GPS data in a wide range of practical and Earth Science applications. The author is also indebted to *P. Tétreault* and *Y. Mireault* of Geodetic Survey Div., Natural Resource Canada, who have kindly reviewed this contribution and provided the author with valuable suggestions and comments.

7. References

Beutler, G., J. Kouba, and T. Springer, 1995, Combining the Orbits of the IGS Analysis Centers, *Bull. Geod. 69*, pp. 200-222.

Herring, T. A. and D. Dong, 1994, Measurement of diurnal and semidiurnal rotational variations and tidal parameters of Earth, *Jour. Geoph. Res., Vol. 99*, No. B9, September, pp. 18051-18071.

IERS, 1996, IERS Conventions (1996), *IERS Technical Note 21*, (ed. D.D. McCarthy), IERS Central Bureau, (http://maia.usno.navy.mil/conventions.html).

IERS, 2000, IERS Conventions (2000), *Draft of IERS Conventions 2000*, (ed. D.D. McCarthy and G. Petit), IERS Central Bureau, (http://maia.usno.navy.mil/conv2000.html).

Kouba, J., Y. Mireault, G. Beutler and T. Springer, 1998, A Discussion of IGS Solutions and Their Impact on Geodetic and Geophysical Applications, *GPS Solutions, Vol. 2, No. 2*, pp. 3-15.

Kouba, J., G. Beutler and M. Rothacher, 2000, IGS Combined and Contributed Earth Rotation Parameter Solutions, in Polar Motion Historical and Scientific Problems IAU Colloquium 178, *The Astronomical Society of Pacific Series Conference Series, Vol. 208*, (Eds S. Dick, D.D. McCarthy and B. Luzum), pp. 277-302.

Kouba, J., 2002, Sub-daily Earth Rotation Parameters and the International GPS Service Orbit/Clock Solution Products, accepted for publications, *Studia Geophysica et Geodetica 46 (2002)*, pp. 9-25.

Neilan, R.E., P.A. Van Scoy and J.F. Zumberge (eds), 1996, Proceedings of 1996 IGS Analysis Center Workshop, *IGS Central Bureau*, March 19-21, Silver Spring, Maryland, U.S.A.(ftp://igscb.jpl.nasa.gov/igscb/resource/pubs/ac_ws96a.pdf).

Ray, R.D., D.J. Steinberg, B.F. Chao and D.E. Cartwright, 1994, Diurnal and Semidiurnal Variations in Earth's Rotation Rate Induced by Oceanic Tides, *Science, Vol. 264*, May 6, pp. 630-632.

Rothacher, M., 1998, Recent Contributions of GPS to Earth Rotation and Reference Frames, Habilitationsschrift Philosophisch-naturwissenshaftliche Fakultaet der Universitaet Bern, *Druckerei der Universitaet Bern*, May 6.

Rothacher, M., G. Beutler, R. Weber, and J. Hefty, 2001, High-frequency variations in Earth rotation from Global Positioning System data, *Jour. Geoph. Res., Vol. 106,* No. B7, July, pp. 13711-13738.

New IGS Clock Alignment Results

International GPS Service
Network, Data and Analysis Center Workshop 2002

K. Senior
U.S. Naval Observatory

8-11 April 2002

Outline

- IGS/BIPM Pilot Project overview
- IGS combined clock products
- IGS time scale algorithm
- Clock results

- Analysis of day-boundary discontinuities
- Accuracy and precision study
- Conclusions

IGS/BIPM Pilot Project Overview

- Goal: develop strategies to exploit geodetic techniques for improved global time/freq. comparisons
- Began March 1998 with participation of >35 groups
- IGS contributes:
  - global tracking network
  - standards for operating geodetic stations
  - efficient data delivery system
  - state-of-the-art analysis groups/methods/products
- BIPM contributes expertise in:
  - high-accuracy metrological standards/measurements
  - timing calibration methods
  - time scale algorithms
  - formation & dissemination of UTC

Potential of Geodetic Methods for Timing

- Common view method *(Allan & Weiss, 1980)*
  - single-freq. C/A pseudorange data only
  - requires coordinated tracking schedules
  - common mode errors approximately cancel
  - accuracy few ns at 5-d intervals

- Geodetic method
  - dual-freq. pseudorange + carrier phase data
  - model all effects explicitly & accurately
  - sub-cm positioning at 1-d intervals implies **sub-ns** potential for time transfer

IGS Combined Clock Products

- IGS analysis centers contributing:
  - CODE *Center for Orbit Determination in Europe, AIUB, Switzerland*
  - ESOC *European Space Operations Center, ESA, Germany*
  - GFZ *GeoForschungsZentrum, Germany*
  - JPL *Jet Propulsion Laboratory, USA*
  - NRCan *Natural Resources Canada, Canada*
  - USNO *U.S. Naval Observatory, USA*
- Since Nov. 2000
- 5-minute intervals for all satellites and ~ 175 stations
- Supports autonomous point positioning at few cm level
- Time scale limited by daily alignment to GPS Time

Mix of Clocks in IGS Combined Clock Products

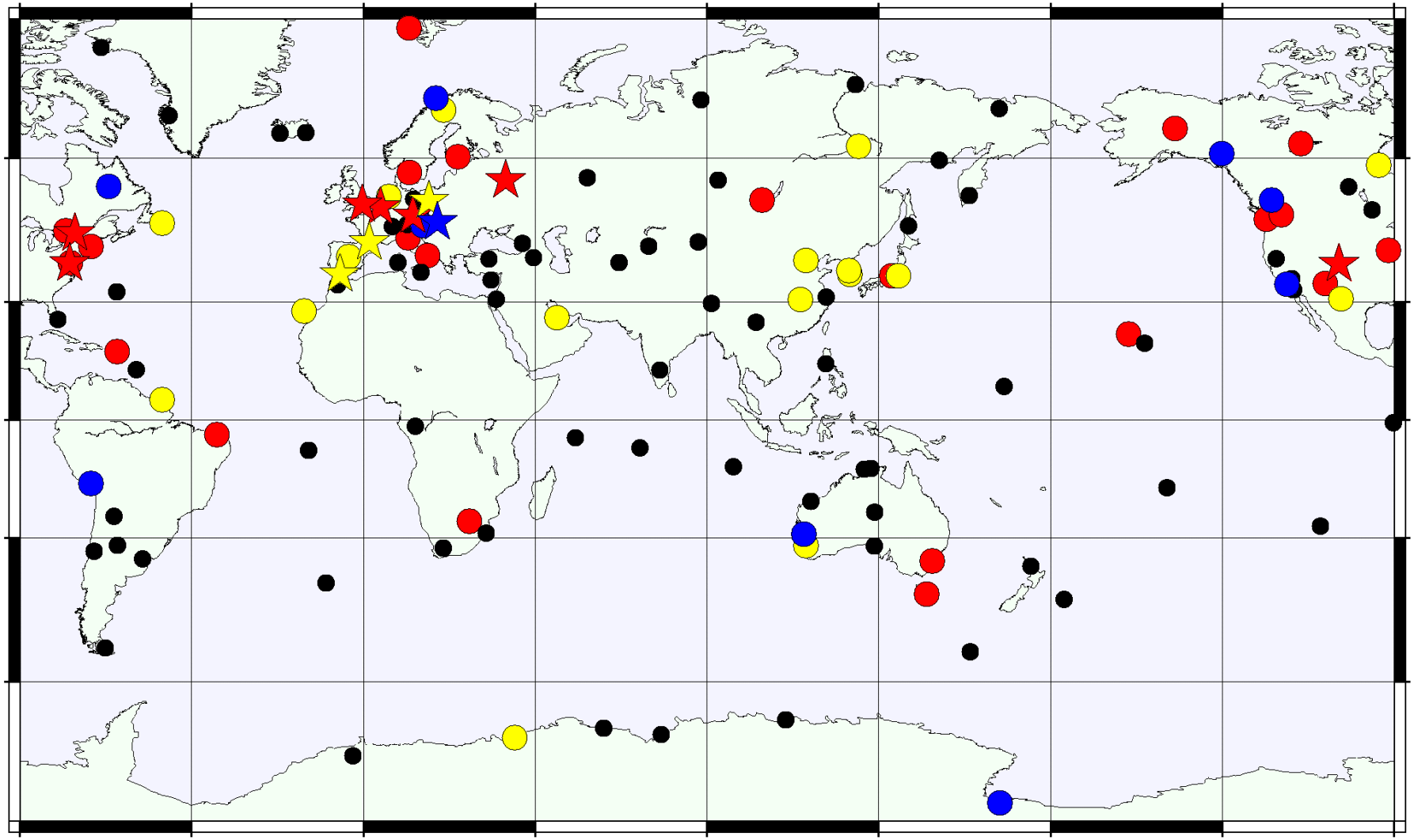

masers
cesiums
rubidiums
crystals
☆ timing labs in IGS

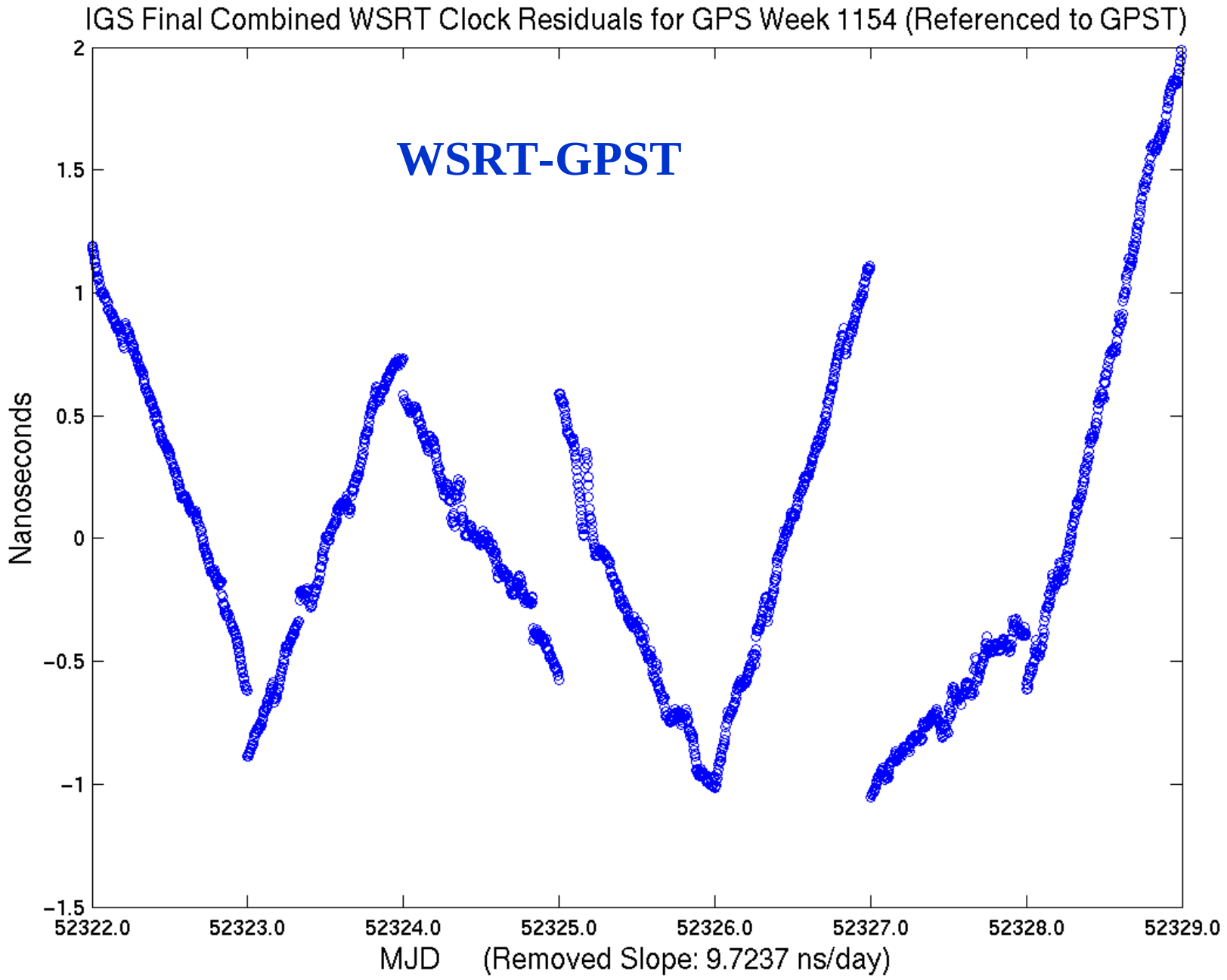
IGS Final Combined WSRT Clock Residuals for GPS Week 1154 (Referenced to GPST)
WSRT-GPST
Nanoseconds
2
1.5
1
0.5
0
−0.5
−1
−1.5
52322.0
52323.0
52324.0
52325.0
52326.0
52327.0
52328.0
52329.0
MJD
(Removed Slope: 9.7237 ns/day)

New IGS Time Scale: Filter Highlights

- Uses IGS clock RINEX format
- Can support IGS move to real-time processing
- Kalman continuous filter implementation
  - formulated as a frequency ensemble
  - deterministic model: rates, drifts
  - process noise capabilities: White FM, Random Walk FM, Random Run FM
- Dynamic weighting of frequency standards
- Robust outlier detection
- Modular

Clock Model

$$\begin{bmatrix} r(t_{i+1}) \\ d(t_{i+1}) \end{bmatrix} = \begin{bmatrix} 1 & t \\ 0 & 1 \end{bmatrix} \begin{bmatrix} r(t_i) \\ d(t_i) \end{bmatrix} + \begin{bmatrix} e_1(t_{i+1}) \\ e_2(t_{i+1}) \end{bmatrix}$$

$$y(t) = \begin{bmatrix} 1 & 0 \end{bmatrix} \begin{bmatrix} r(t) \\ d(t) \end{bmatrix} + h(t)$$

1st order polynomial fit to frequency data, (i.e. rate and drift.)

$$E[h^2] = \frac{a_0}{t}$$

spd. White FM

spd. Random Walk FM

$$E[ee^T] = \begin{bmatrix} a_{-1}t + a_{-2}\frac{t^3}{3} & a_{-2}\frac{t^2}{2} \\ a_{-2}\frac{t^2}{2} & a_{-2}t \end{bmatrix}$$

spd. Random Run FM

Frequency Scale Equation

At t_{i+1}, detrend the clocks relative to the new ensemble using estimates of rate & drift at t_i :

$$y_k(t_{i+1}) = y_k^{\mathrm{GPST}}(t_{i+1}) - \sum_{j=1}^{N} w_j(t_{i+1}) \left[y_j^{\mathrm{GPST}}(t_{i+1}) - \left(\begin{bmatrix} 1 & t \\ 0 & 1 \end{bmatrix} \begin{bmatrix} r_j(t_i) \\ d_j(t_i) \end{bmatrix} \right)_1 \right]$$

The new frequency scale relative to the old reference (GPST) is then formed as:

$$y_{\mathrm{GPST}}^{\mathrm{IGST}}(t_{i+1}) \overset{\mathrm{def}}{=} \sum_{j=1}^{N} w_j(t_{i+1}) \left[y_j^{\mathrm{GPST}}(t_{i+1}) - r_j(t_{i+1}) \right]$$

Weighting Scheme

- Nominal weights (unnormalized) determined in the short term using Allan Variance measures:

$$w_j = \frac{1}{\max\left\{ t_1 \cdot s^2_{y_j}(t_1),\quad t_2 \cdot s^2_{y_j}(t_2),\quad t_3 \cdot s^2_{y_j}(t_3),\quad \right\}}$$

$$t_1 = 1200\text{s},\quad t_1 = 10{,}200\text{s},\quad t_3 = 12\text{hours}$$

- 1st iteration: uses 1 d of data with GPST as reference
- 2nd iteration: uses 7 d of data with IGS(R)T as reference
- Upper limit of weights enforced as:

$$w_j < \max\left\{ 0.1,\ \frac{2.5}{\#\,\text{masers}},\ \frac{2.5}{\#\,\text{clocks}} \right\}$$

Integrate and Steer to GPS Time

- Integrate $y_{\mathrm{GPST}}^{\mathrm{IGST}}$ to get a time series $x_{\mathrm{GPST}}^{\mathrm{IGST}}$ of GPST vs. IGST

- Slowly steer this quantity to zero using a 3-state (phase, rate, drift) LQG algorithm

  - gain chosen *(30-40 d time constant):*

$$G = \begin{bmatrix} 6.323\times10^{-6} & 2.261\times10^{-5} & 3.963\times10^{-4} \end{bmatrix}$$

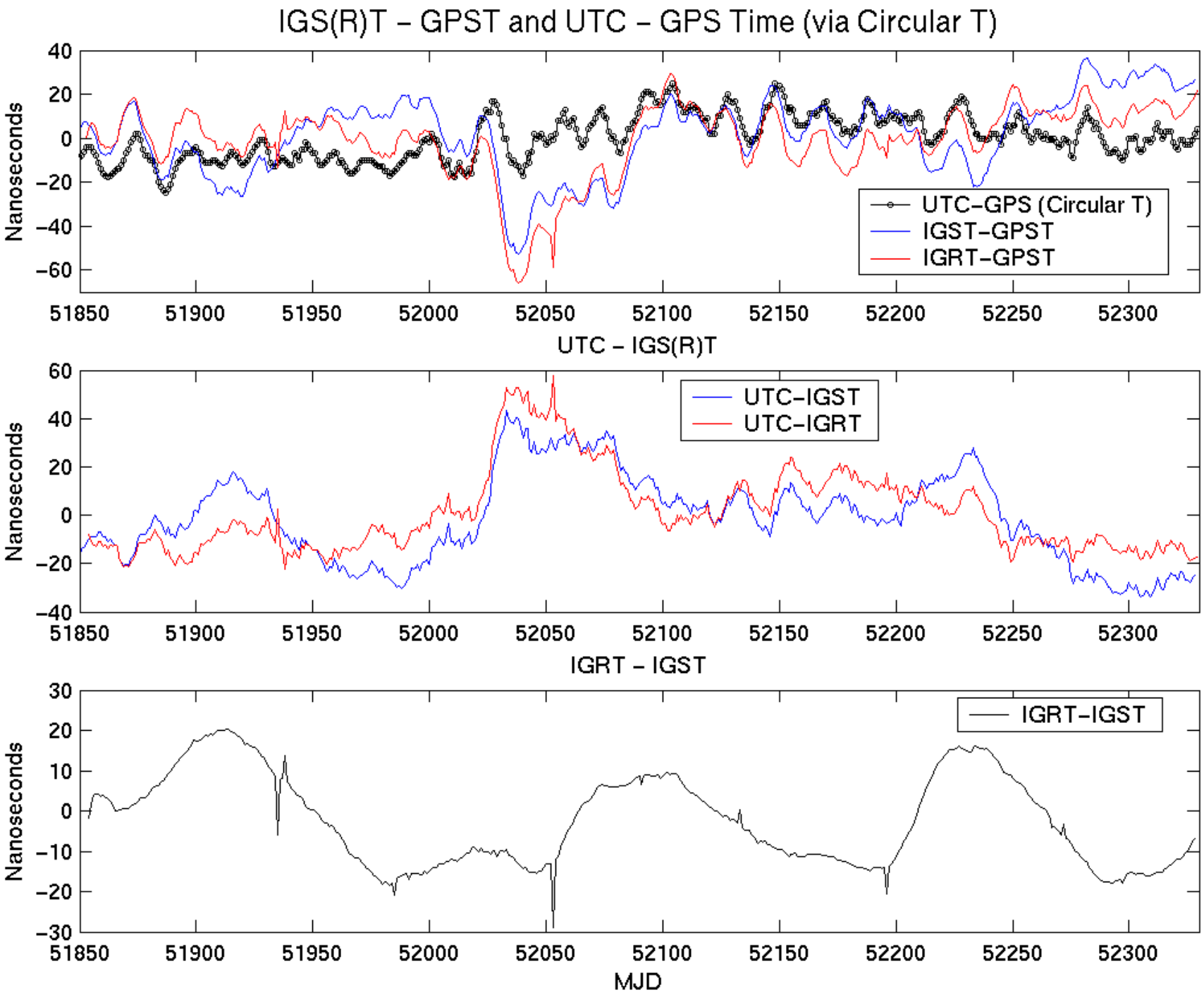
IGS(R)T – GPST and UTC – GPS Time (via Circular T)
Nanoseconds
40
20
0
−20
−40
−60
UTC−GPS (Circular T)
IGST−GPST
IGRT−GPST
51850
51900
51950
52000
52050
52100
52150
52200
52250
52300
UTC – IGS(R)T
Nanoseconds
60
40
20
0
−20
−40
UTC−IGST
UTC−IGRT
IGRT – IGST
Nanoseconds
30
20
10
0
−10
−20
−30
IGRT−IGST
MJD

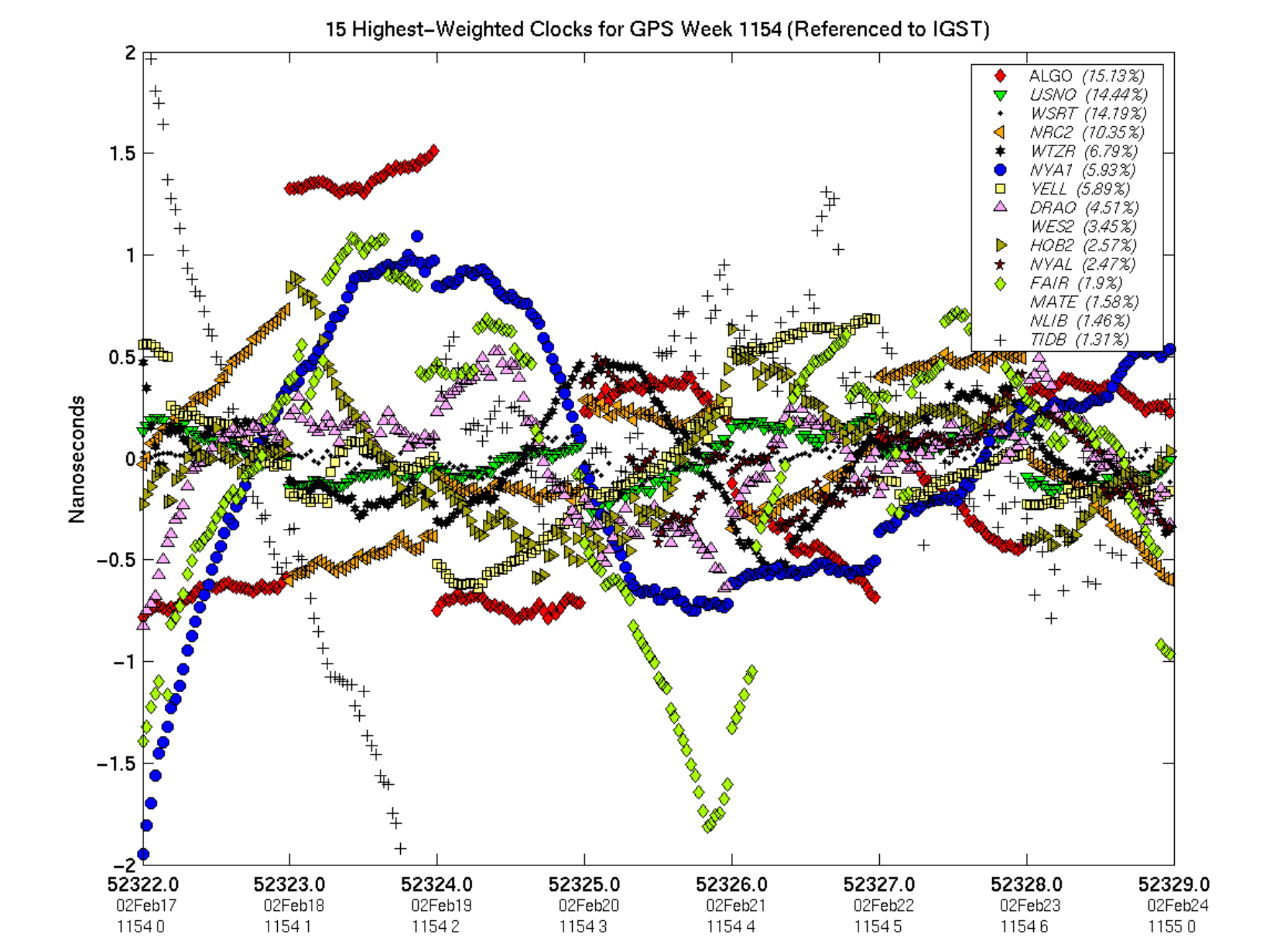
15 Highest–Weighted Clocks for GPS Week 1154 (Referenced to IGST)
Nanoseconds
2
1.5
1
0.5
0
−0.5
−1
−1.5
−2
ALGO (15.13%)
USNO (14.44%)
WSRT (14.19%)
NRC2 (10.35%)
WTZR (6.79%)
NYA1 (5.93%)
YELL (5.89%)
DRAO (4.51%)
WES2 (3.45%)
HOB2 (2.57%)
NYAL (2.47%)
FAIR (1.9%)
MATE (1.58%)
NLIB (1.46%)
TIDB (1.31%)
52322.0 02Feb17 1154 0
52323.0 02Feb18 1154 1
52324.0 02Feb19 1154 2
52325.0 02Feb20 1154 3
52326.0 02Feb21 1154 4
52327.0 02Feb22 1154 5
52328.0 02Feb23 1154 6
52329.0 02Feb24 1155 0

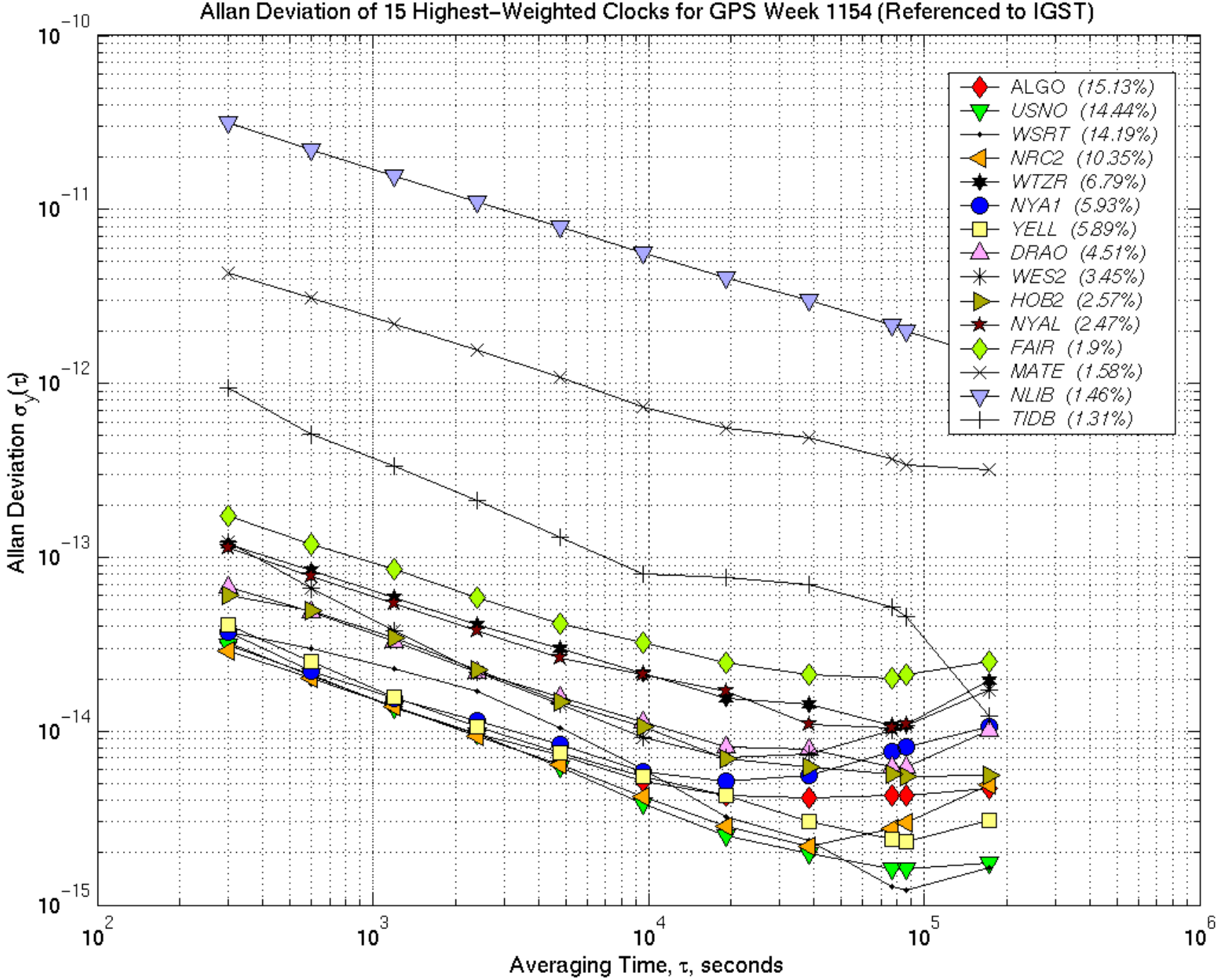
Allan Deviation of 15 Highest−Weighted Clocks for GPS Week 1154 (Referenced to IGST)
Allan Deviation σy(τ)
Averaging Time, τ, seconds
ALGO (15.13%)
USNO (14.44%)
WSRT (14.19%)
NRC2 (10.35%)
WTZR (6.79%)
NYA1 (5.93%)
YELL (5.89%)
DRAO (4.51%)
WES2 (3.45%)
HOB2 (2.57%)
NYAL (2.47%)
FAIR (1.9%)
MATE (1.58%)
NLIB (1.46%)
TIDB (1.31%)

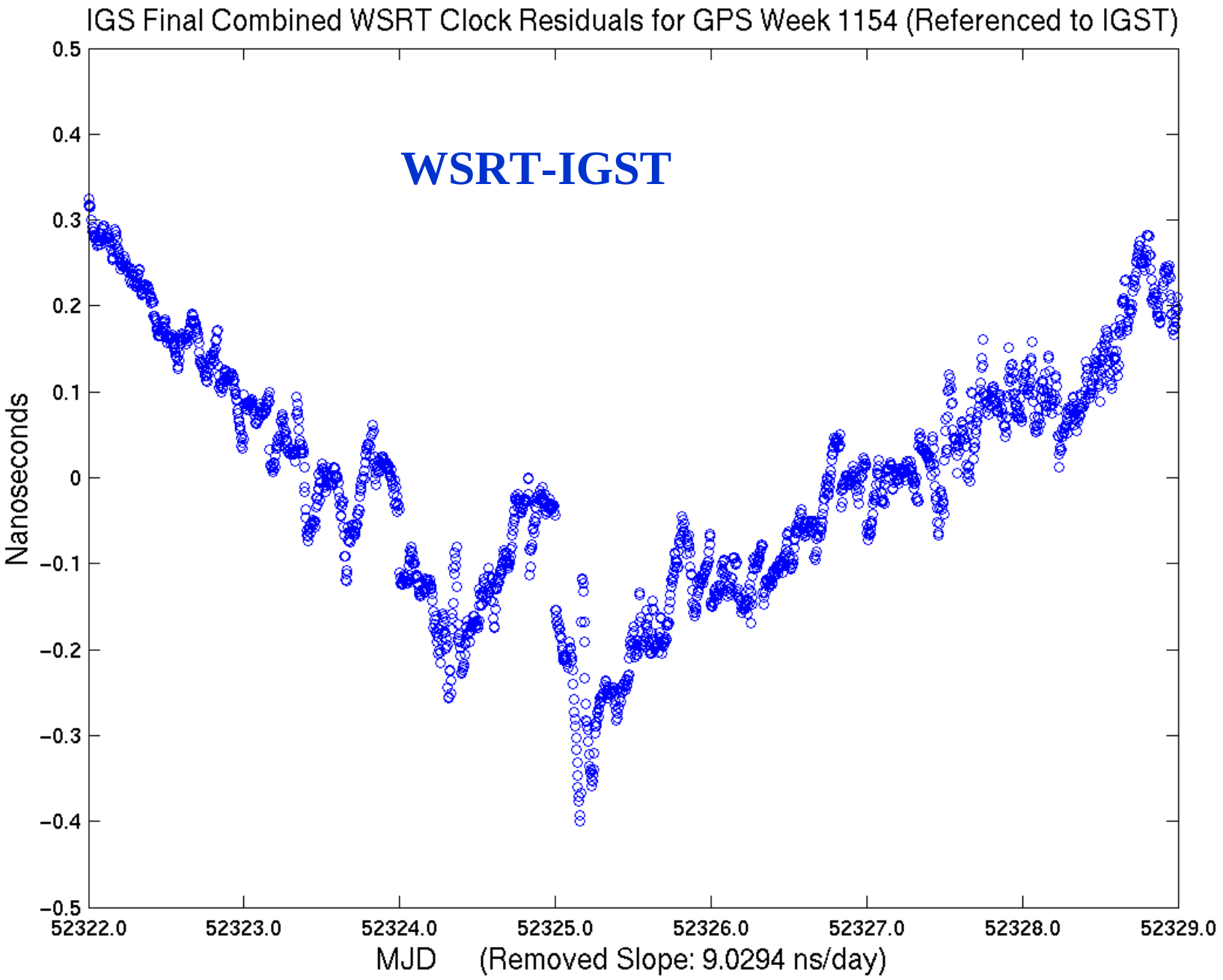
IGS Final Combined WSRT Clock Residuals for GPS Week 1154 (Referenced to IGST)
WSRT-IGST
Nanoseconds
0.5
0.4
0.3
0.2
0.1
0
−0.1
−0.2
−0.3
−0.4
−0.5
52322.0
52323.0
52324.0
52325.0
52326.0
52327.0
52328.0
52329.0
MJD
(Removed Slope: 9.0294 ns/day)

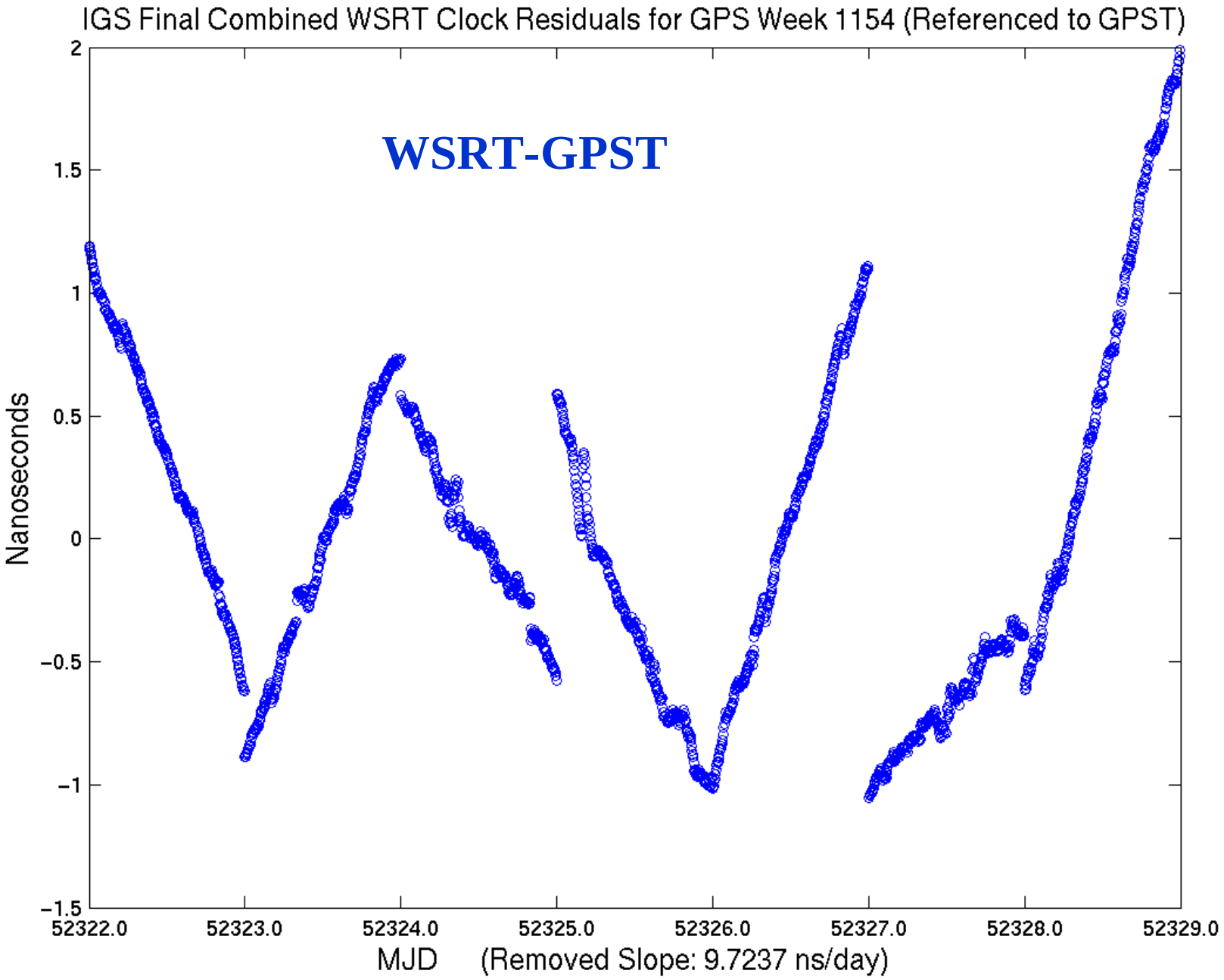
IGS Final Combined WSRT Clock Residuals for GPS Week 1154 (Referenced to GPST)
WSRT-GPST
Nanoseconds
2
1.5
1
0.5
0
−0.5
−1
−1.5
52322.0
52323.0
52324.0
52325.0
52326.0
52327.0
52328.0
52329.0
MJD
(Removed Slope: 9.7237 ns/day)

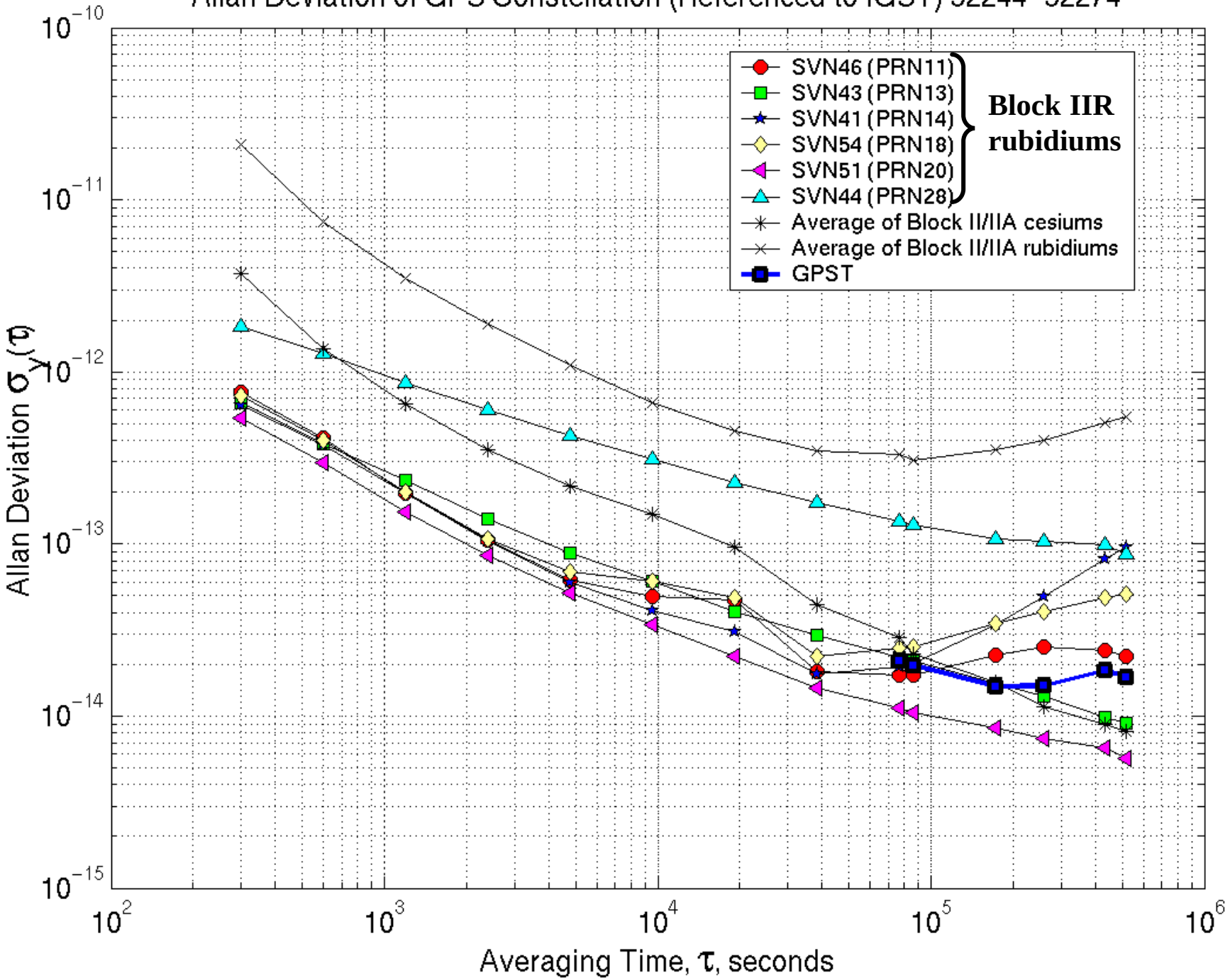
Allan Deviation of GPS Constellation (Referenced to IGST) 52244–52274
SVN46 (PRN11)
SVN43 (PRN13)
SVN41 (PRN14)
SVN54 (PRN18)
SVN51 (PRN20)
SVN44 (PRN28)
Block IIR rubidiums
Average of Block II/IIA cesiums
Average of Block II/IIA rubidiums
GPST
Allan Deviation σy(τ)
Averaging Time, τ, seconds
10−10
10−11
10−12
10−13
10−14
10−15
10^2
10^3
10^4
10^5
10^6

Accuracy Considerations

- Pseudorange data ($s \approx 1\text{m}$)
  - necessary to separate clock offset and phase ambiguities
  - determines absolute accuracy (mod calibration biases) of clock estimates over analysis span
- Carrier phase data ($s \approx 1\text{cm}$)
  - determines detailed time variation (i.e., stability) of clock
- Clock estimate formal error
  - $s \approx 100\text{-}125\text{ps}$ for 24-hour analysis arc
- Can assess true accuracy by comparing clock estimates at boundaries between consecutive *independent* arcs

Day-Boundary Clock Jump Analysis

- Clock estimates of a sub-network of 30 IGS sites for the 15-month period Nov. 2001 – Feb. 2002
  - all equipped with H-Masers
  - referenced to new IGS timescale IGST ~ 10^{-15} at 1 d
- Day-boundary clock discontinuities formed according to:
  - linearly detrended over 2-d span
  - 30 min. before and after day boundary observed
  - formal error of clock jump must be < 500ps
  - rms variation over each day's estimates must be < 150ps
  - jumps > 5ns rejected as outliers

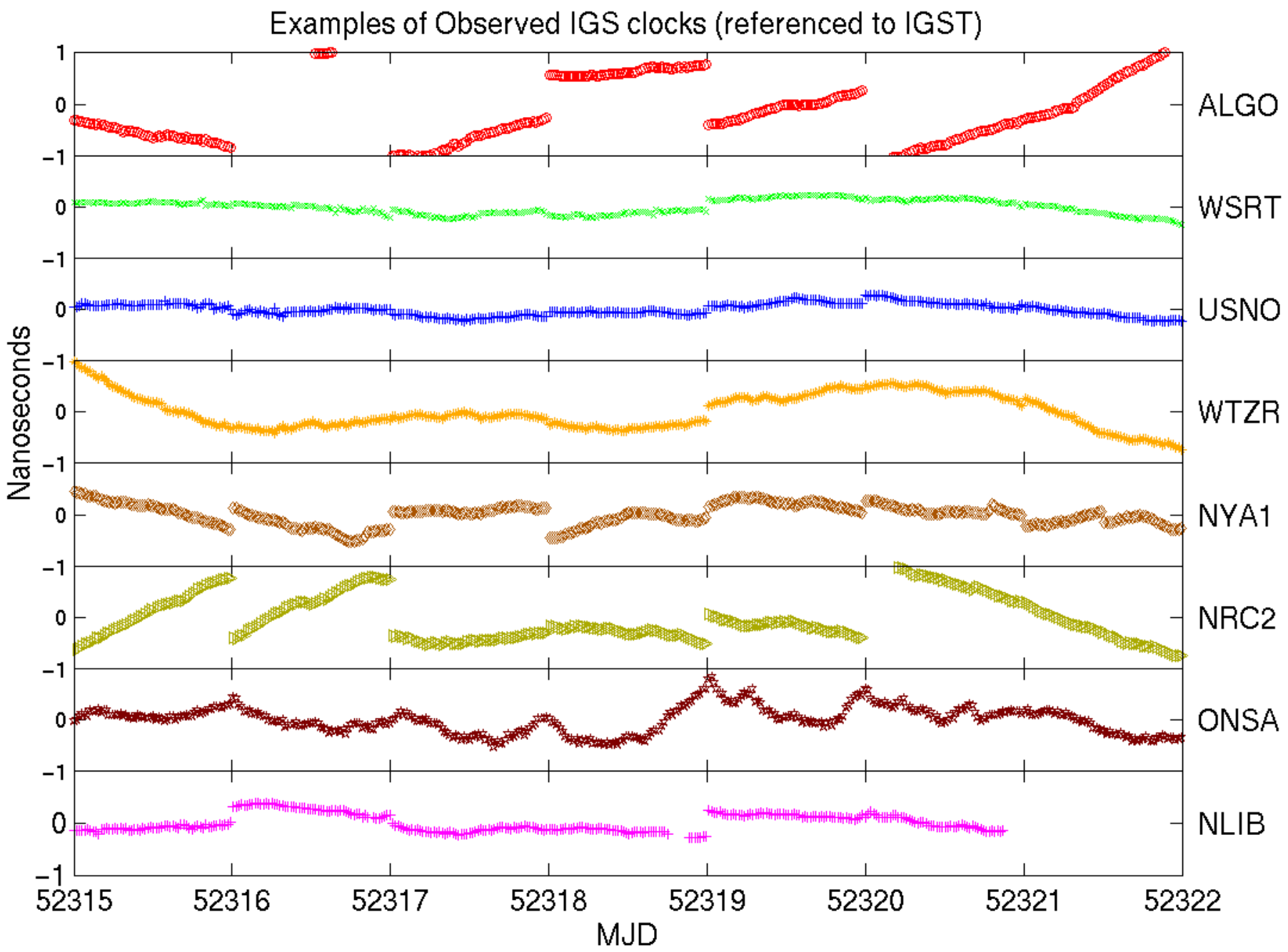
Examples of Observed IGS clocks (referenced to IGST)
Nanoseconds
MJD
ALGO
WSRT
USNO
WTZR
NYA1
NRC2
ONSA
NLIB
52315
52316
52317
52318
52319
52320
52321
52322

Day-Boundary Clock Jumps

- Measure of lower limit on accuracy of time transfer
- Approximately zero-mean & Gaussian
- Variance is highly site-dependent
- rms variation among the 30 stations varies from 170 ps – 1200 ps
- Variance does not depend on receiver/antenna types
- Some sites have seasonal variation of time transfer accuracy
- Performance depends on overall station data quality, especially cable and receiver problems

Day-Boundary Clock Discontinuities Using IGS Combined Clock Products
(Finals for GPS Weeks 1086-1151; Rapids for GPS Weeks 1087-1153)

IGS site	Mean jump (ps)	rms of jumps (ps)	# jumps	Receiver model	Antenna model	Remarks
NOT1	66	80	2	TRIMBLE 4000SSI	TRM29659.00	
GODE	4	173	34	AOA SNR-12 ACT	AOAD/M_T dome	
WTZR	-5	184	301	AOA SNR-8000 ACT	AOAD/M_T	
ONSA	-54	186	66	ASHTECH Z-XII3	AOAD/M_B dome	
BRUS R	-36	207	140	ASHTECH Z-XII3T	ASH701945B_M	
WSRT	-46	222	414	AOA SNR-12 ACT	AOAD/M_T dome	
TIDB	-51	222	172	ASHTECH Z-XII3	AOAD/M_T	
CRO1	73	248	165	ASHTECH Z-XII3	AOAD/M_T	
USNO	7	252	392	AOA SNR-12 ACT	AOAD/M_T	
USUD	-97	256	75	ASHTECH Z-XII3	AOAD/M_T	
NPLD R	-65	280	92	ASHTECH Z-XII3T	AOAD/M_T	
WES2	-43	361	242	mixed types	AOAD/M_T	all data
	-74	400	143	AOA ROGUE SNR-8000	AOAD/M_T	until 29 Jun 2001
	2	295	99	ASHTECH UZ-12	AOAD/M_T	starting 27 Jul 2001
IRKT	-117	375	123	AOA ROGUE SNR-8000	AOAD/M_T	
NYAL	-57	378	209	AOA BENCHMARK ACT	AOAD/M_B dome	
NLIB	161	411	90	AOA ROGUE SNR-8000	AOAD/M_T dome	
FAIR R	-97	422	125	AOA SNR-8100 ACT	AOAD/M_T dome	
PIE1	100	442	290	AOA ROGUE SNR-8000	AOAD/M_T	
MATE	-7	444	271	TRIMBLE 4000SSI	TRM29659.00	all data
	-71	605	95			18 Apr - 24 Sep 2001
	27	325	176			all other times
NYA1	-81	456	364	AOA BENCHMARK ACT	ASH701073.1 dome	has several large outliers
	-63	323	356			edit 8 very large outliers
ALBH R	32	534	222	AOA BENCHMARK ACT	AOAD/M_T dome	
DRAO	37	551	406	AOA BENCHMARK ACT	AOAD/M_T	
YELL	-30	613	382	AOA BENCHMARK ACT	AOAD/M_T	all data
	-63	810	155			winters (1 Dec - 22 Mar)
	-7	431	227			summers (all other times)
MEDI R	-94	680	40	TRIMBLE 4000SSI	TRM29659.00	
ALGO	29	691	389	AOA BENCHMARK ACT	AOAD/M_T	all data
	14	1097	124			winters (1 Dec - 22 Mar)
	36	373	265			summers (all other times)
AMC2 R	-40	718	156	AOA SNR-12 ACT	AOAD/M_T	all data
	-8	329	150			edit 6 very large outliers
HOB2	-79	816	359	AOA ICS-4000Z ACT	AOAD/M_T	distinct time-variable behavior
FORT	373	858	61	AOA ROGUE SNR-8000	AOAD/M_TA_NGS	
NRC1	-28	1009	418	AOA SNR-12 ACT	AOAD/M_T	all data
	-29	1514	159			winters (1 Dec - 22 Mar)
	-27	485	259			summers (all other times)
METS	53	1105	64	ASHTECH Z-XII3	AOAD/M_B	
KOKB R	227	1223	18	AOA SNR-8100 ACT	AOAD/M_T dome	

R with the site name designates results from IGS Rapid clocks; all others from IGS Finals. Rapids clocks are used only when a station is unavailable in the Finals or when $> 25\%$ jumps are available in the Rapids.

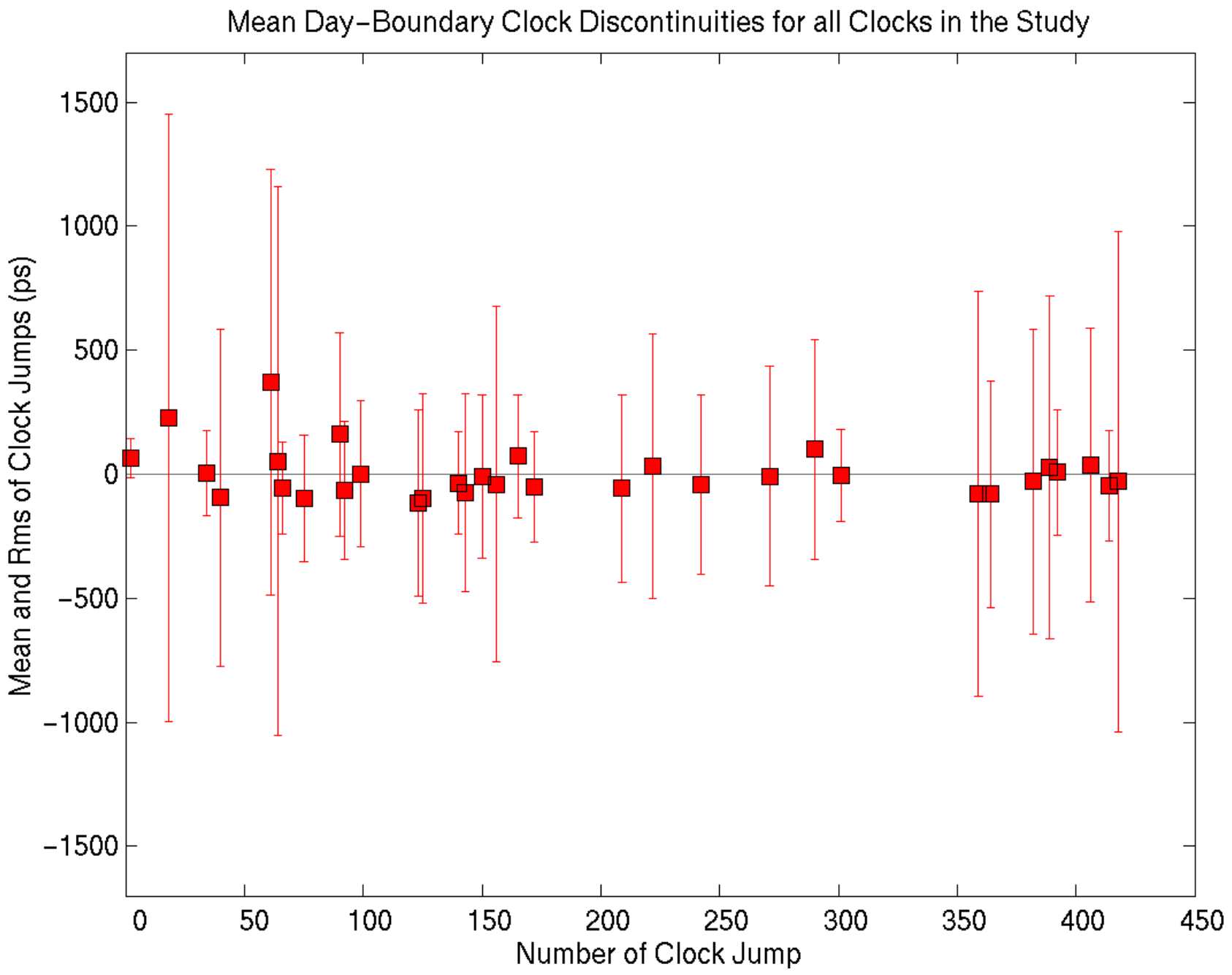
Mean Day−Boundary Clock Discontinuities for all Clocks in the Study
Mean and Rms of Clock Jumps (ps)
1500
1000
500
0
−500
−1000
−1500
0
50
100
150
200
250
300
350
400
450
Number of Clock Jump

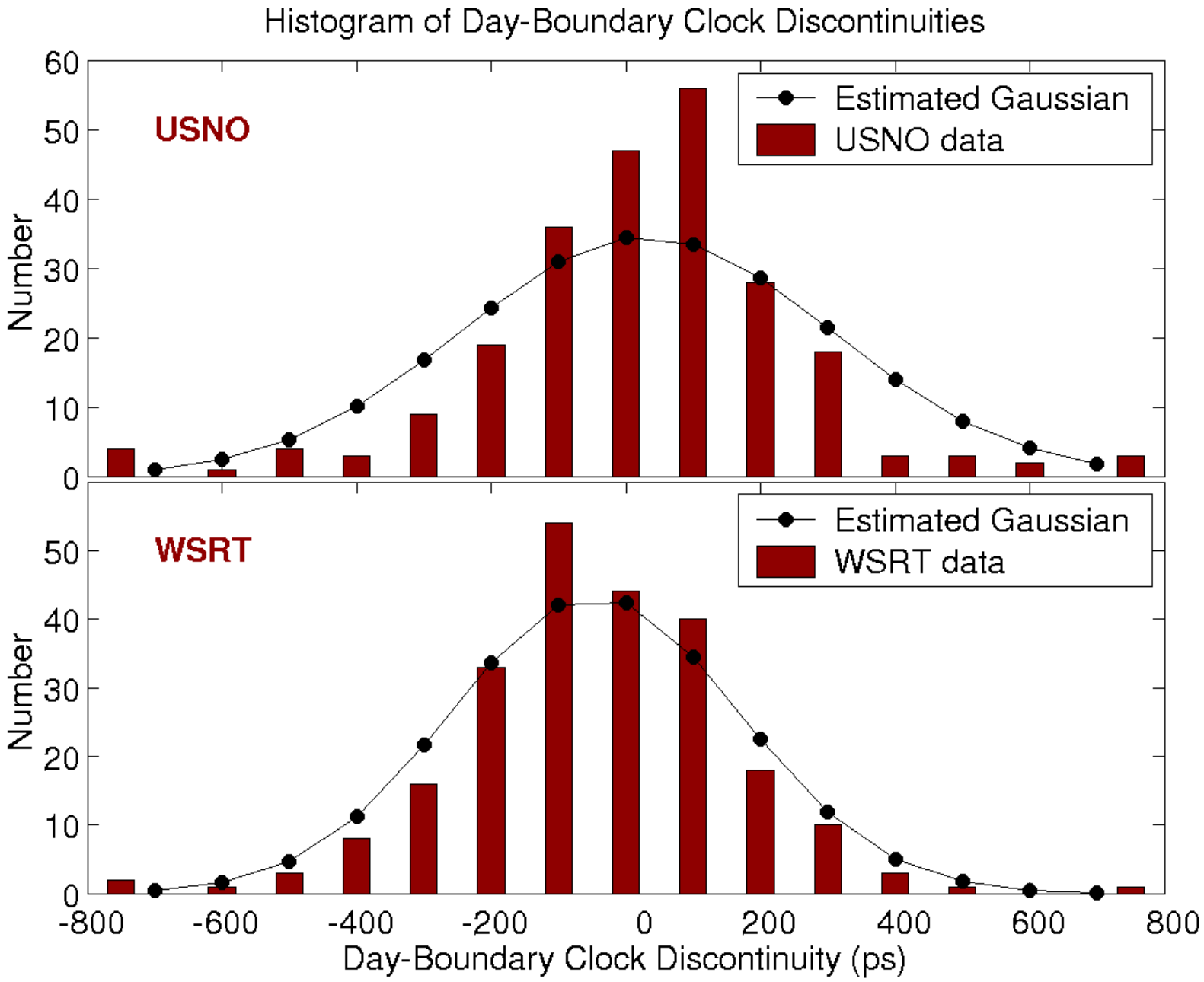
Histogram of Day-Boundary Clock Discontinuities
USNO
Estimated Gaussian
USNO data
WSRT
Estimated Gaussian
WSRT data
Number
Number
0
10
20
30
40
50
60
-800
-600
-400
-200
0
200
400
600
800
Day-Boundary Clock Discontinuity (ps)

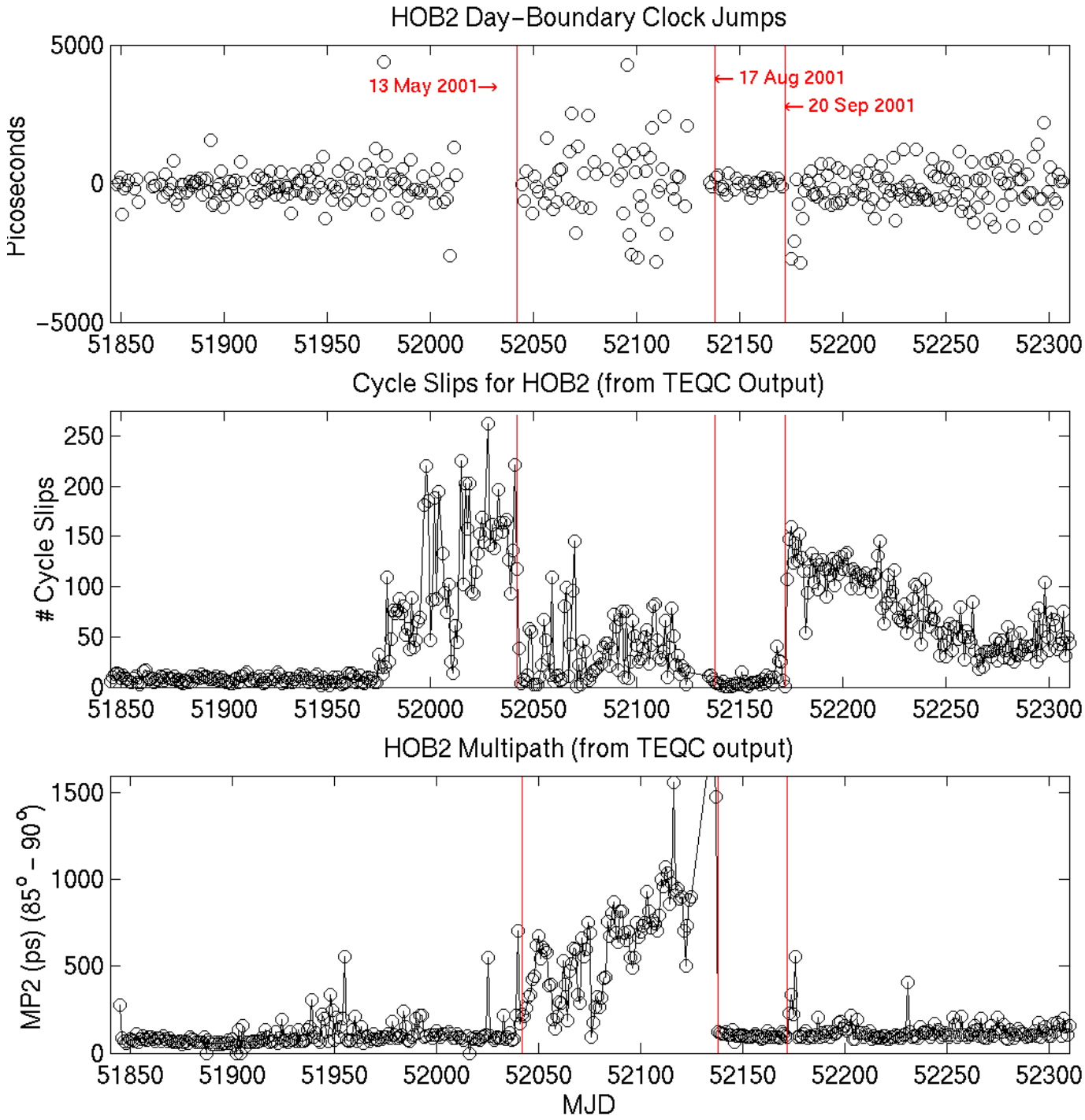
HOB2 Day−Boundary Clock Jumps
Picoseconds
5000
0
−5000
13 May 2001→
← 17 Aug 2001
← 20 Sep 2001
51850
51900
51950
52000
52050
52100
52150
52200
52250
52300
Cycle Slips for HOB2 (from TEQC Output)
Cycle Slips
250
200
150
100
50
0
HOB2 Multipath (from TEQC output)
MP2 (ps) (85° − 90°)
1500
1000
500
0
MJD

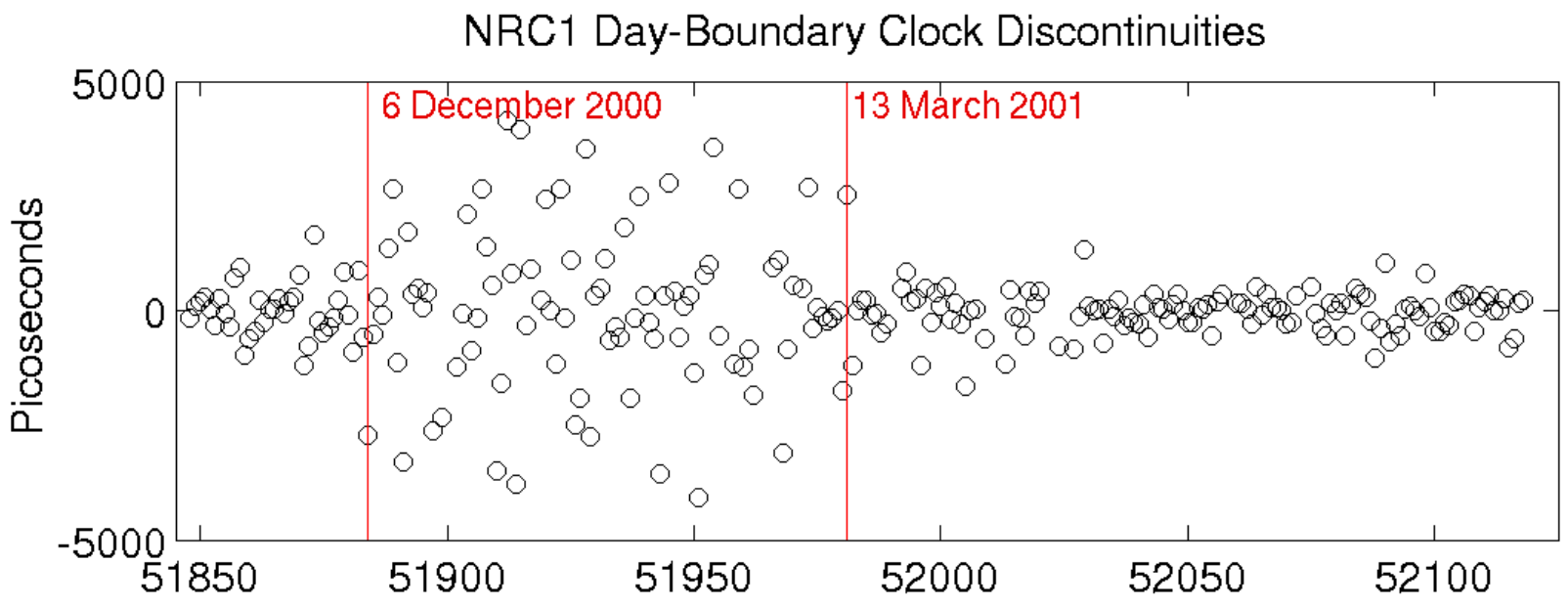
NRC1 Day-Boundary Clock Discontinuities
Picoseconds
5000
0
-5000
6 December 2000
13 March 2001
51850
51900
51950
52000
52050
52100

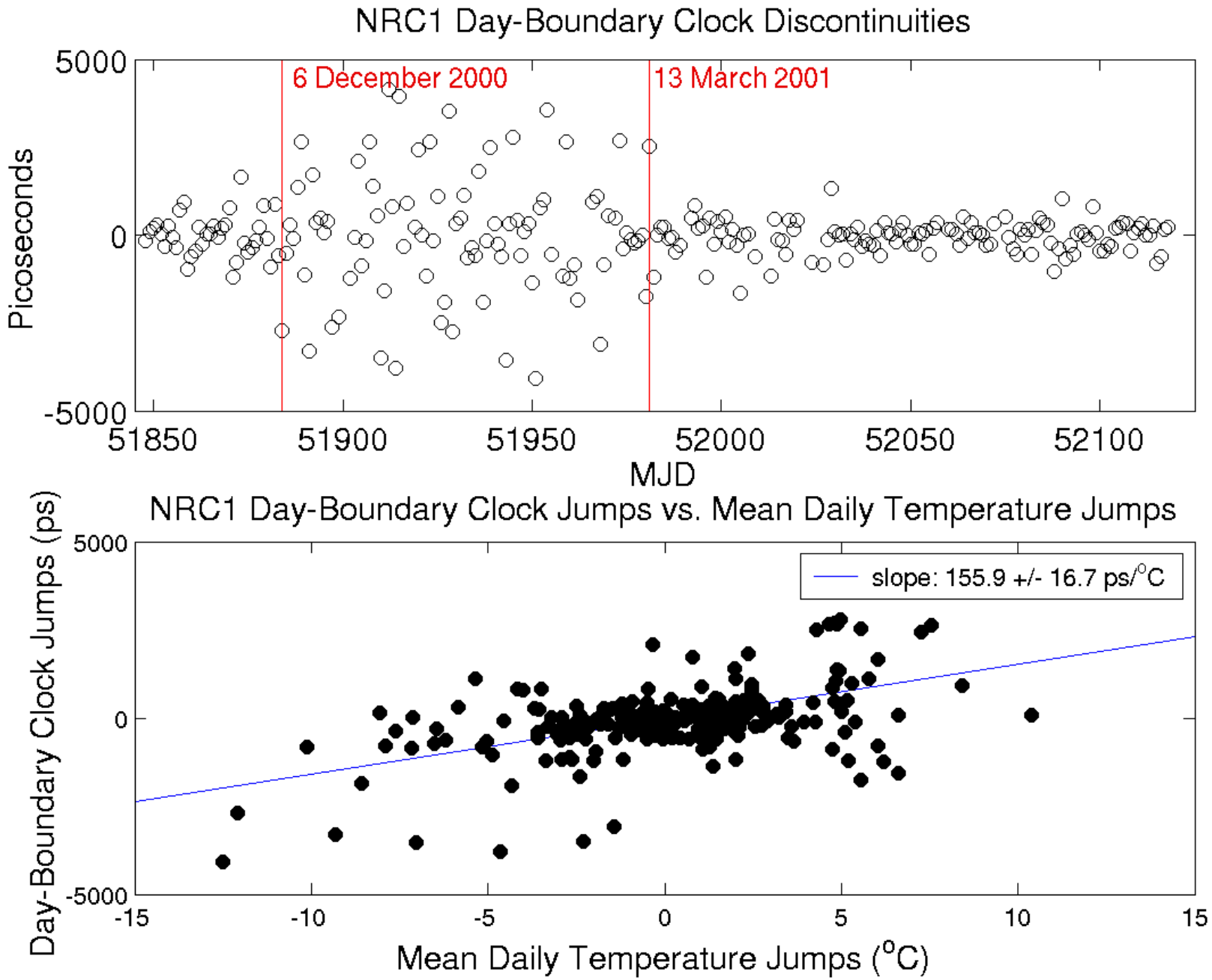
NRC1 Day-Boundary Clock Discontinuities
6 December 2000
13 March 2001
Picoseconds
5000
0
-5000
51850
51900
51950
52000
52050
52100
MJD
NRC1 Day-Boundary Clock Jumps vs. Mean Daily Temperature Jumps
slope: 155.9 +/- 16.7 ps/°C
Day-Boundary Clock Jumps (ps)
5000
0
-5000
-15
-10
-5
0
5
10
15
Mean Daily Temperature Jumps (°C)

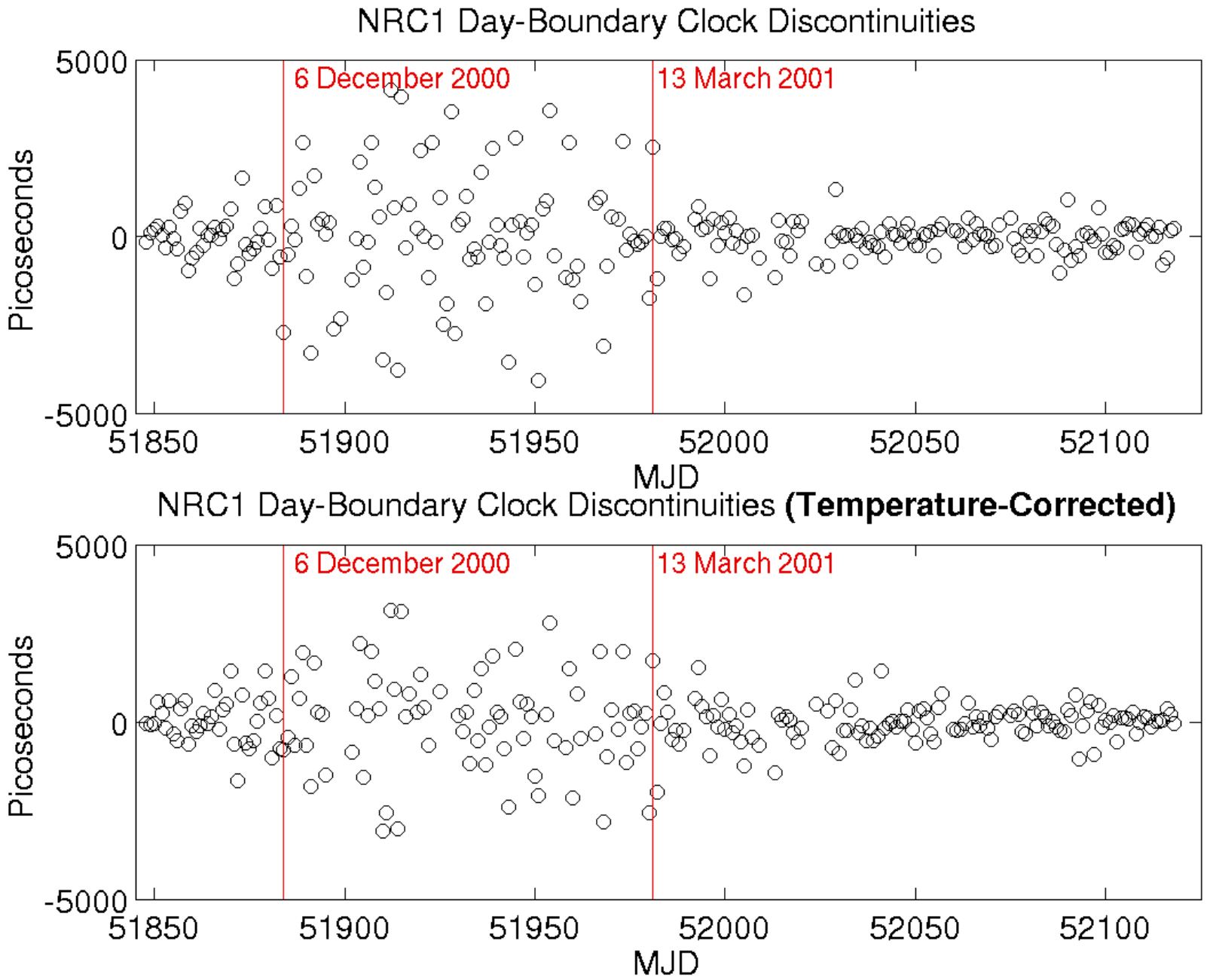
NRC1 Day-Boundary Clock Discontinuities
6 December 2000
13 March 2001
5000
0
-5000
Picoseconds
51850
51900
51950
52000
52050
52100
MJD
NRC1 Day-Boundary Clock Discontinuities (Temperature-Corrected)
6 December 2000
13 March 2001
5000
0
-5000
Picoseconds
51850
51900
51950
52000
52050
52100
MJD

Day-boundary Clock Jumps vs. Temperature Changes
(GPS Weeks 1086-1124)

IGS site	Correl. coeff.	rms resid. (ps)	Slope (ps/°C)		Slope sigma (ps/°C)	# pnts	Range of temp. jumps (°C)
WTZR	0.3615	164	25.3		5.5	145	13.4
FAIR	0.0068	232	0.5		9.7	61	17.6
USNO	**0.0435**	**293**	**3.7**		**6.4**	177	20.1
WES2	0.1137	377	12.2		9.1	139	21.0
ALBH	-0.4167	456	-127.3		35.0	65	8.3
MATE	-0.0520	503	-12.6		19.8	152	12.2
DRAO	-0.2608	555	-54.6		14.6	193	16.8
YELL	0.0671	617	8.6		9.8	172	32.0
ALGO	-0.5973	545	-101.3	*	9.6	202	26.4
NRC1	0.5224	919	155.9	*	16.7	235	22.9
METS	0.1359	1221	80.7		131.6	22	8.6

* slope determination significant to better than 5 sigmas

Temp. Coeff. for Dorne Margolin Antennas

- USNO station:
  - receiver in thermal chamber
  - phase stable antenna cable
  - outside antenna only major uncontrolled component

Previously showed diurnal temperature sensitivity $< 2\ \mathrm{ps}/^{\circ}C$ (Ray & Senior, 2001)

New Results extend analysis to long-term regime: $< 10.1\ \mathrm{ps}/^{\circ}\mathrm{C}$

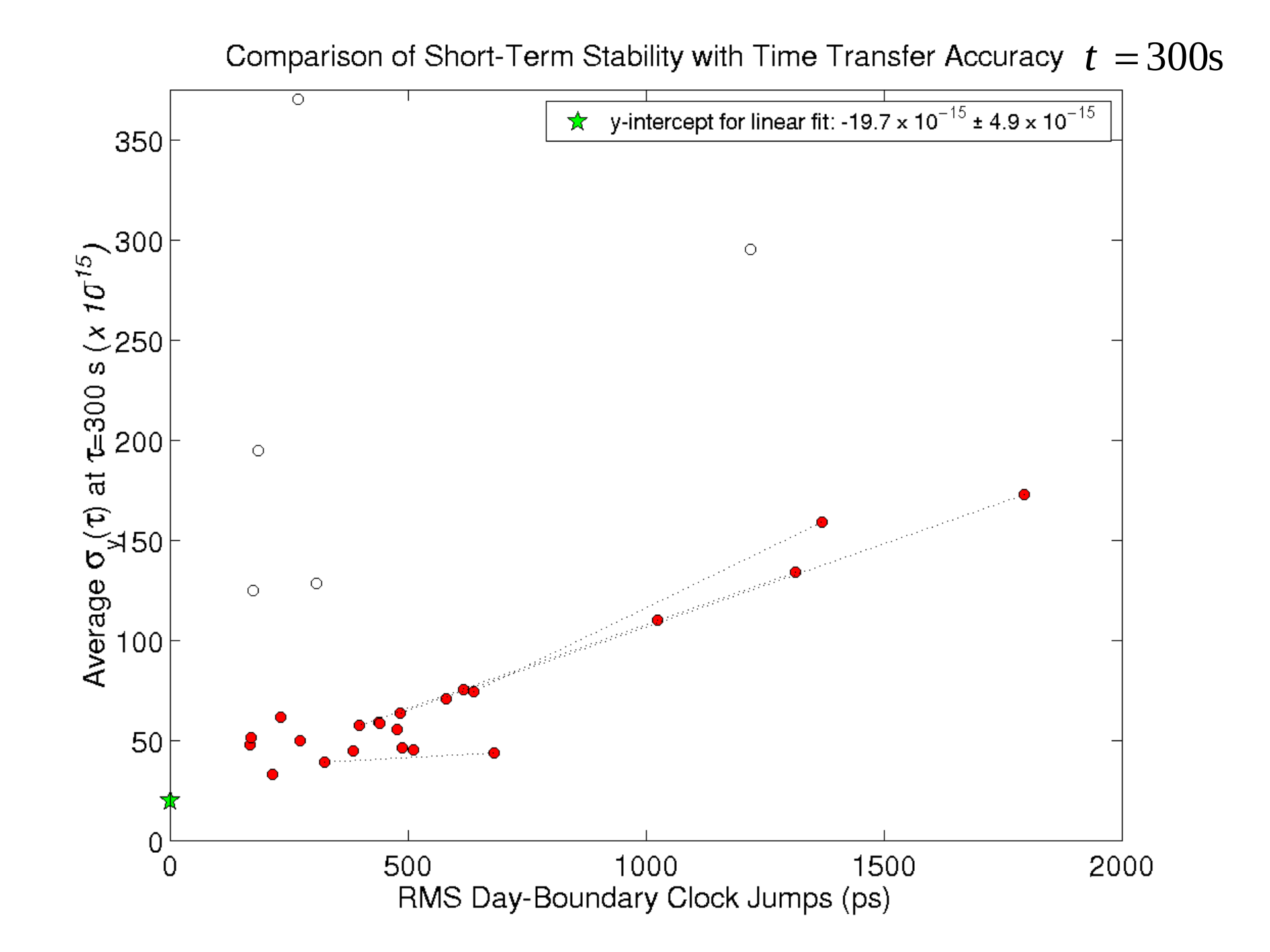
Comparison of Short-Term Stability with Time Transfer Accuracy $t = 300$s
y-intercept for linear fit: -19.7 x 10^-15 ± 4.9 x 10^-15
Average σ_y(τ) at τ=300 s (x 10^-15)
RMS Day-Boundary Clock Jumps (ps)
0
50
100
150
200
250
300
350
0
500
1000
1500
2000

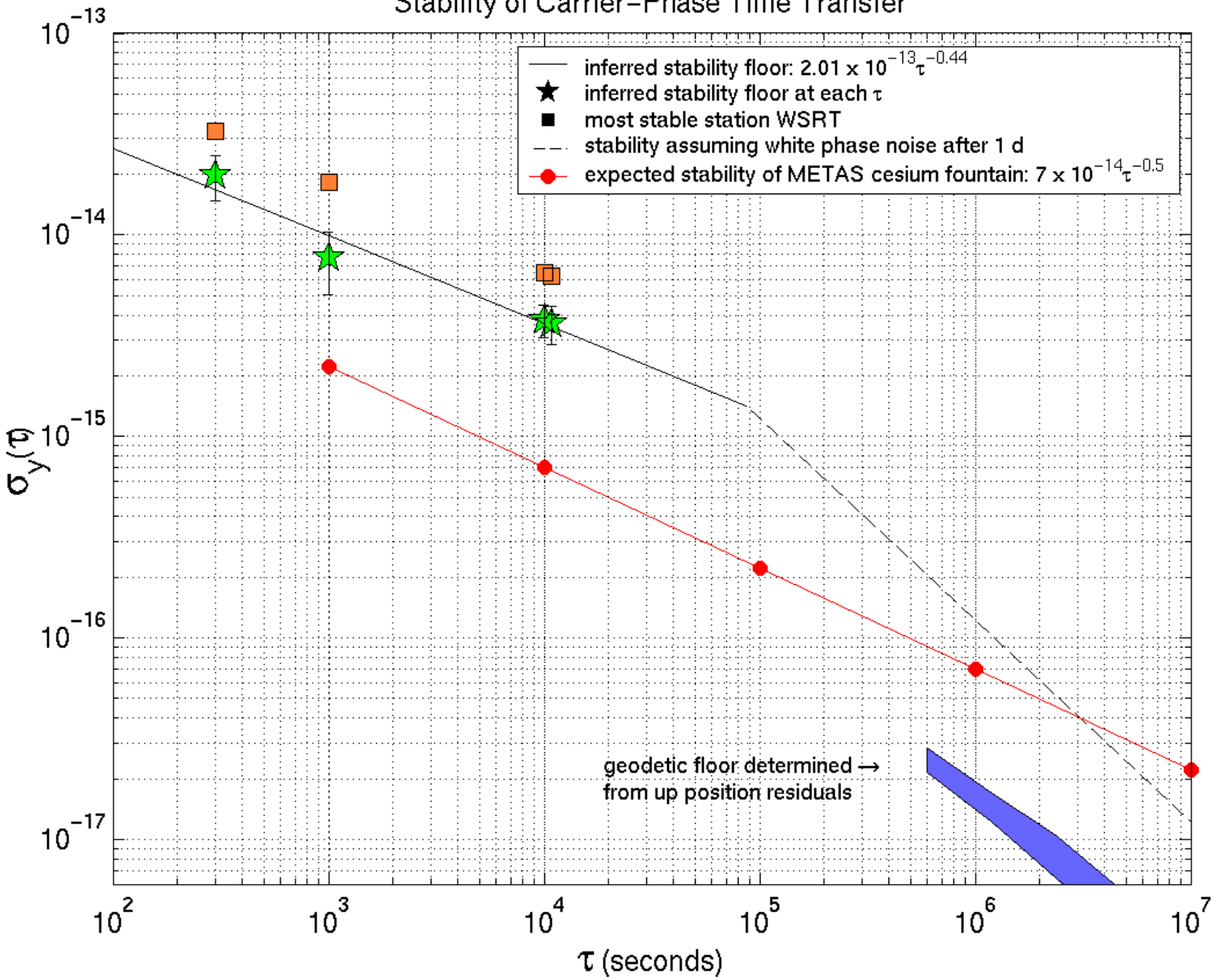
Stability of Carrier−Phase Time Transfer
inferred stability floor: 2.01 x 10^−13 τ^−0.44
inferred stability floor at each τ
most stable station WSRT
stability assuming white phase noise after 1 d
expected stability of METAS cesium fountain: 7 x 10^−14 τ^−0.5
geodetic floor determined →
from up position residuals
σy(τ)
τ (seconds)
10^−13
10^−14
10^−15
10^−16
10^−17
10^2
10^3
10^4
10^5
10^6
10^7

Accuracy & Stability Conclusions

- Time transfer accuracy highly site dependent
  - varies from formal error level (115ps) to nearly 10 times larger
  - does not depend on antenna/receiver choices
  - related to local site effects (temperature, cable conditions, RFI, multipath, etc.)

- Some sites show large temporal changes in accuracy
  - HOB2 probably due to antenna cable problems
  - NRC1 & ALGO seasonal; partly due to temperature
  - YELL also seasonal, but not directly due to temperature.
  - MATE variations probably related to receiver problems
  - NYA1 & AMC2 have very large outliers (RFI?)

- Long-term temperature sensitivity of clock estimates for a Dorne Margolin antenna now determined at $3.7 \pm 6.4\ \mathrm{ps}/^{o}C$

Accuracy & Stability Conclusions *(cont.)*

- Inferred short-term stability floor of time transfer determined for intervals less than 1 d:
  - much better than implied by formal errors
  - $2\times10^{-13}t^{-0.5}$ *(i.e. random walk in phase)*

- Stability > 1 d probably improves as t^{-1} *(white phase noise)* until geodetic instabilities intervene
- Fundamental stability floor probably limited by vertical positioning errors (correlated) of ~ 10 mm for 1 d

Future Directions

- IGS clock densification
  - include IGS clocks not already in combinations (~10 masers; ~8 cesiums)
  - include timing labs not in the IGS (e.g, LPTF, ROAH)
- Newer receivers (e.g., Ashtech Z-12T) and IGS network upgrades
- Links to TAI and predicted TAI
- Future use in TAI

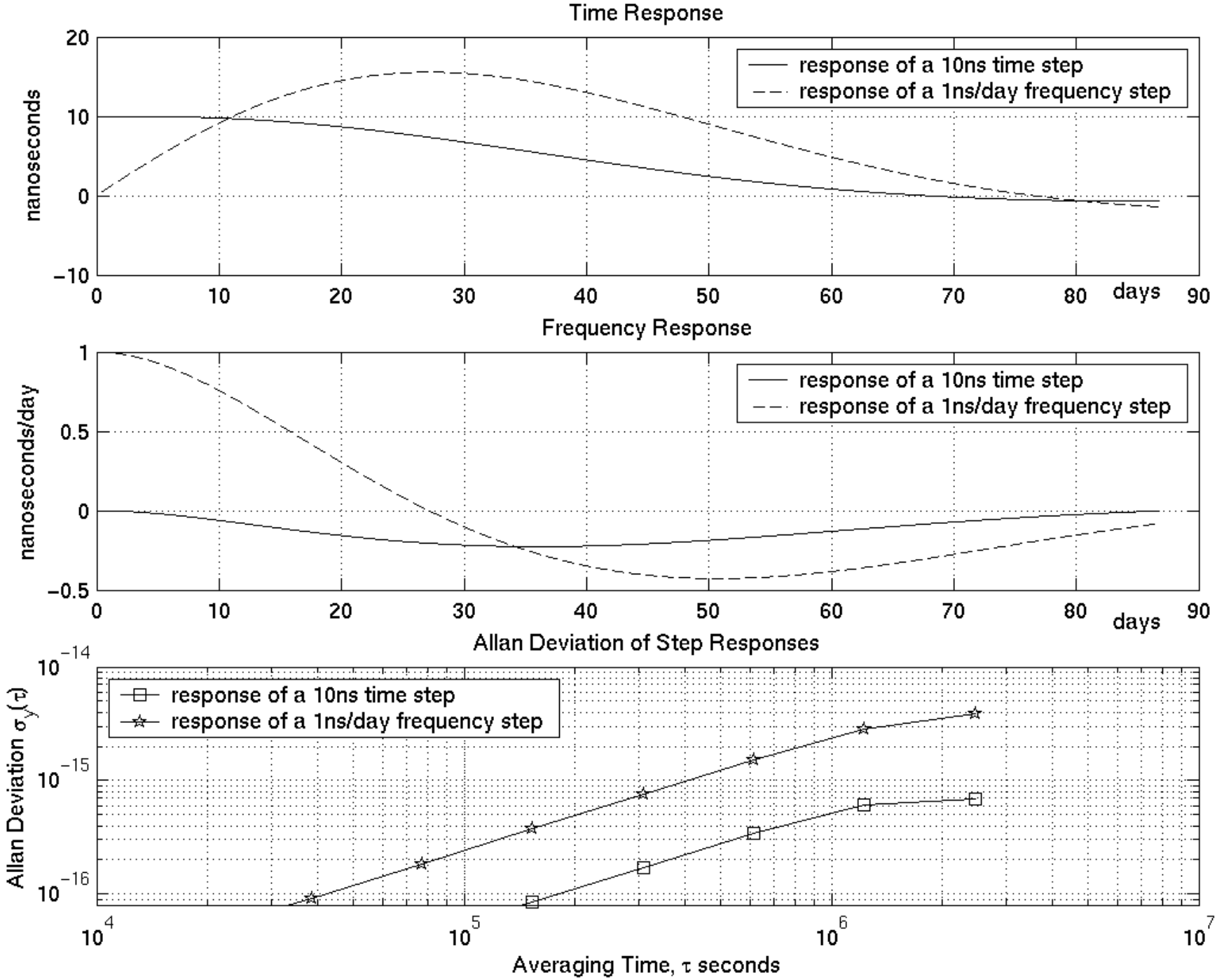
Time Response
nanoseconds
20
10
0
−10
0
10
20
30
40
50
60
70
80
90
days
response of a 10ns time step
response of a 1ns/day frequency step
Frequency Response
nanoseconds/day
1
0.5
0
−0.5
0
10
20
30
40
50
60
70
80
90
days
response of a 10ns time step
response of a 1ns/day frequency step
Allan Deviation of Step Responses
Allan Deviation $\sigma_y(\tau)$
10^{-14}
10^{-15}
10^{-16}
10^4
10^5
10^6
10^7
Averaging Time, τ seconds
response of a 10ns time step
response of a 1ns/day frequency step

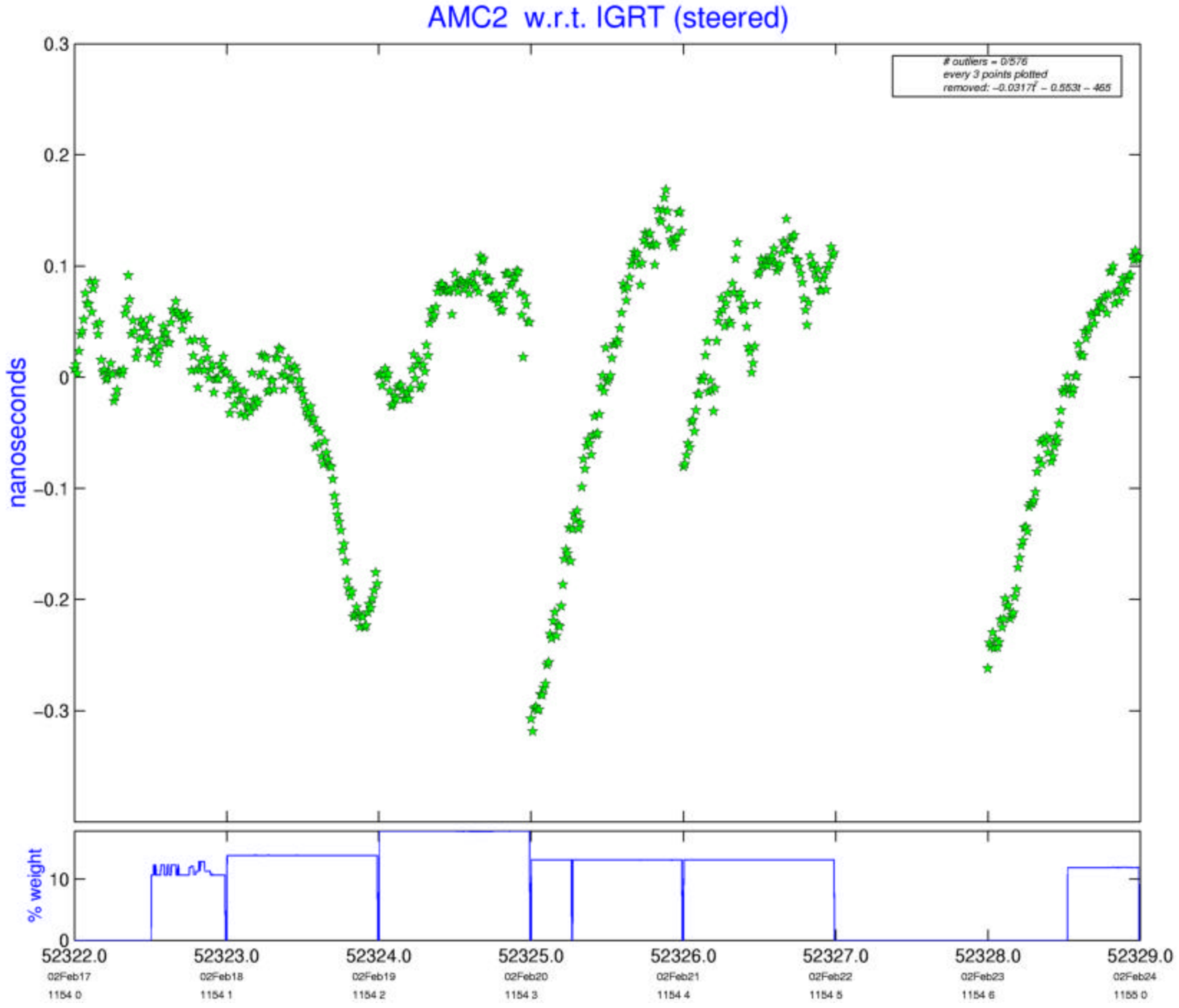
AMC2 w.r.t. IGRT (steered)
outliers = 0/576
every 3 points plotted
removed: −0.0317t² − 0.553t − 465
nanoseconds
0.3
0.2
0.1
0
−0.1
−0.2
−0.3
% weight
10
0
52322.0
52323.0
52324.0
52325.0
52326.0
52327.0
52328.0
52329.0
02Feb17
02Feb18
02Feb19
02Feb20
02Feb21
02Feb22
02Feb23
02Feb24
1154 0
1154 1
1154 2
1154 3
1154 4
1154 5
1154 6
1155 0

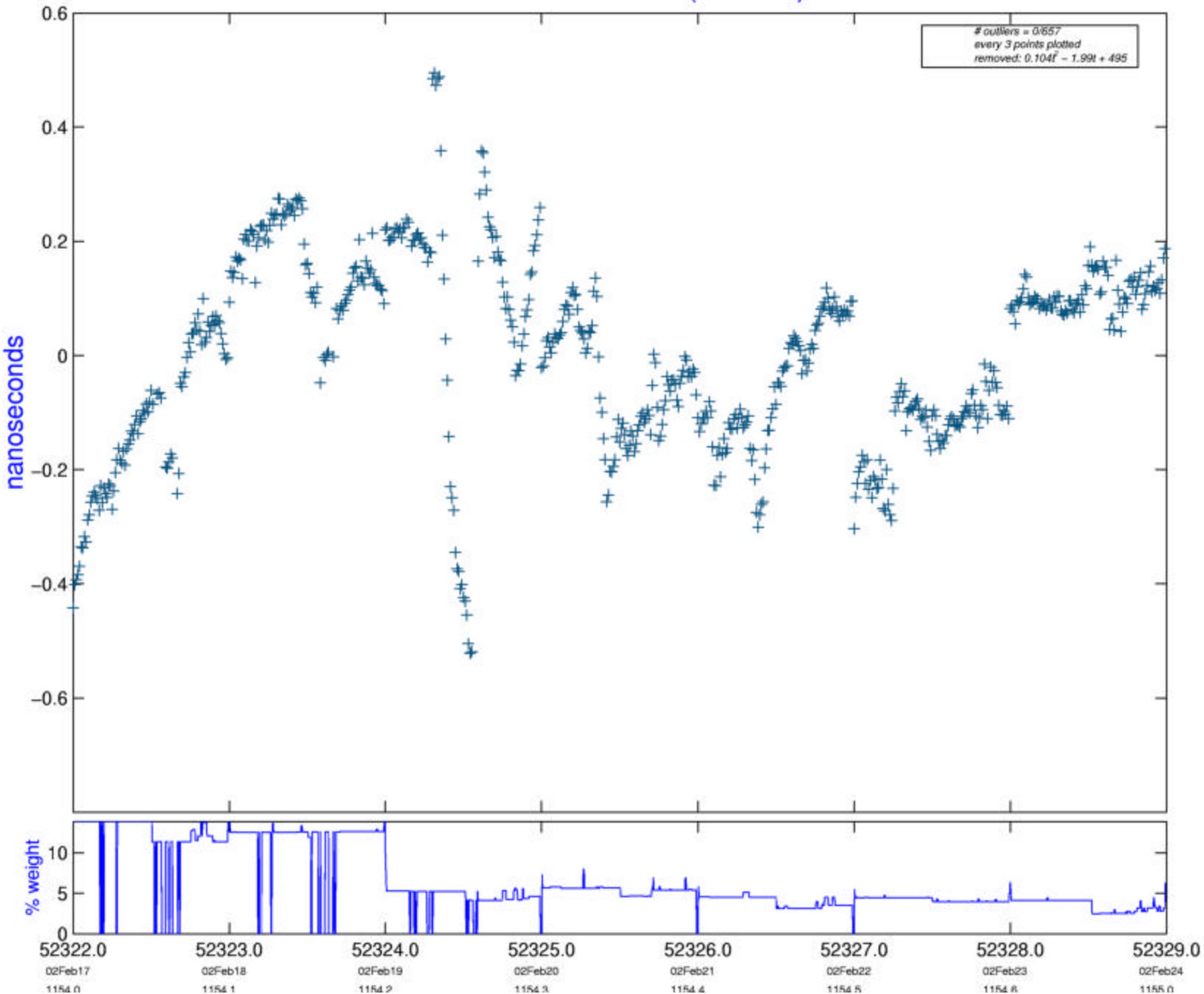
BRUS w.r.t. IGRT (steered)
outliers = 0/657
every 3 points plotted
removed: 0.104t² − 1.99t + 495
nanoseconds
0.6
0.4
0.2
0
−0.2
−0.4
−0.6
% weight
10
5
0
52322.0
52323.0
52324.0
52325.0
52326.0
52327.0
52328.0
52329.0
02Feb17
02Feb18
02Feb19
02Feb20
02Feb21
02Feb22
02Feb23
02Feb24
1154.0
1154.1
1154.2
1154.3
1154.4
1154.5
1154.6
1155.0

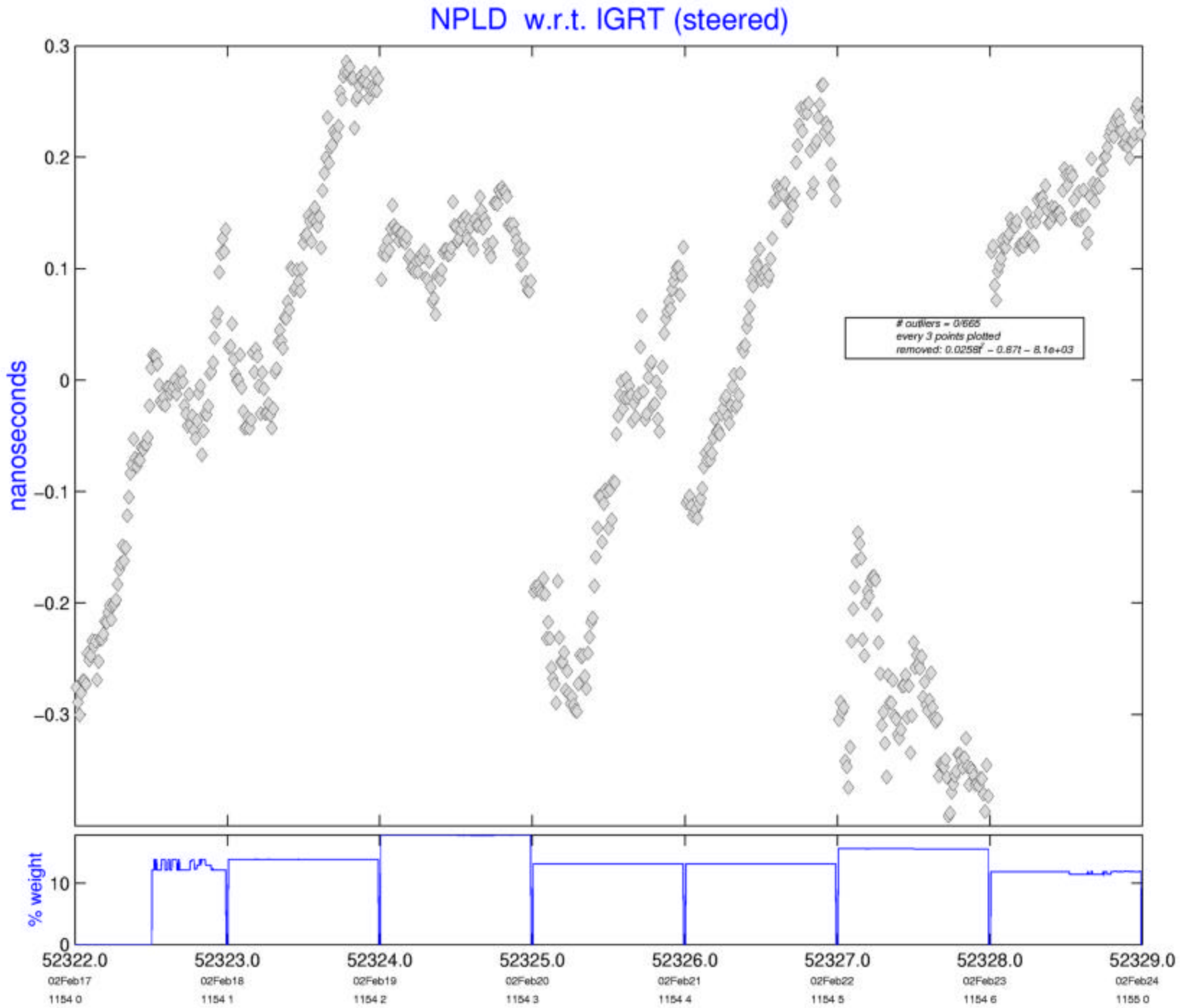
NPLD w.r.t. IGRT (steered)
nanoseconds
0.3
0.2
0.1
0
−0.1
−0.2
−0.3
outliers = 0/665
every 3 points plotted
removed: 0.0258t² − 0.87t − 8.1e+03
% weight
10
0
52322.0
02Feb17
1154 0
52323.0
02Feb18
1154 1
52324.0
02Feb19
1154 2
52325.0
02Feb20
1154 3
52326.0
02Feb21
1154 4
52327.0
02Feb22
1154 5
52328.0
02Feb23
1154 6
52329.0
02Feb24
1155 0

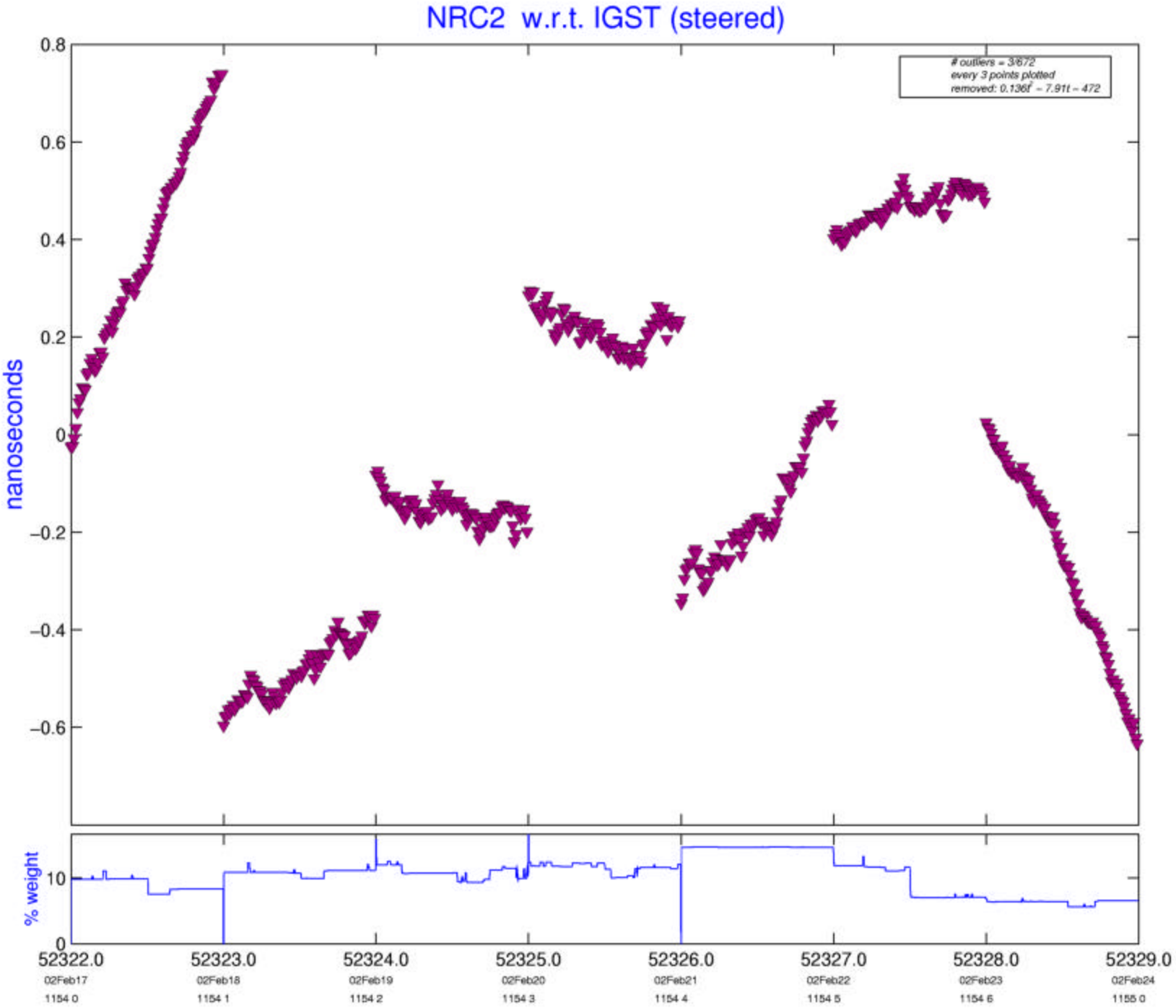
NRC2 w.r.t. IGST (steered)
outliers = 3/672
every 3 points plotted
removed: 0.136t^2 − 7.91t − 472
nanoseconds
0.8
0.6
0.4
0.2
0
−0.2
−0.4
−0.6
% weight
10
0
52322.0
52323.0
52324.0
52325.0
52326.0
52327.0
52328.0
52329.0
02Feb17
02Feb18
02Feb19
02Feb20
02Feb21
02Feb22
02Feb23
02Feb24
1154 0
1154 1
1154 2
1154 3
1154 4
1154 5
1154 6
1155 0

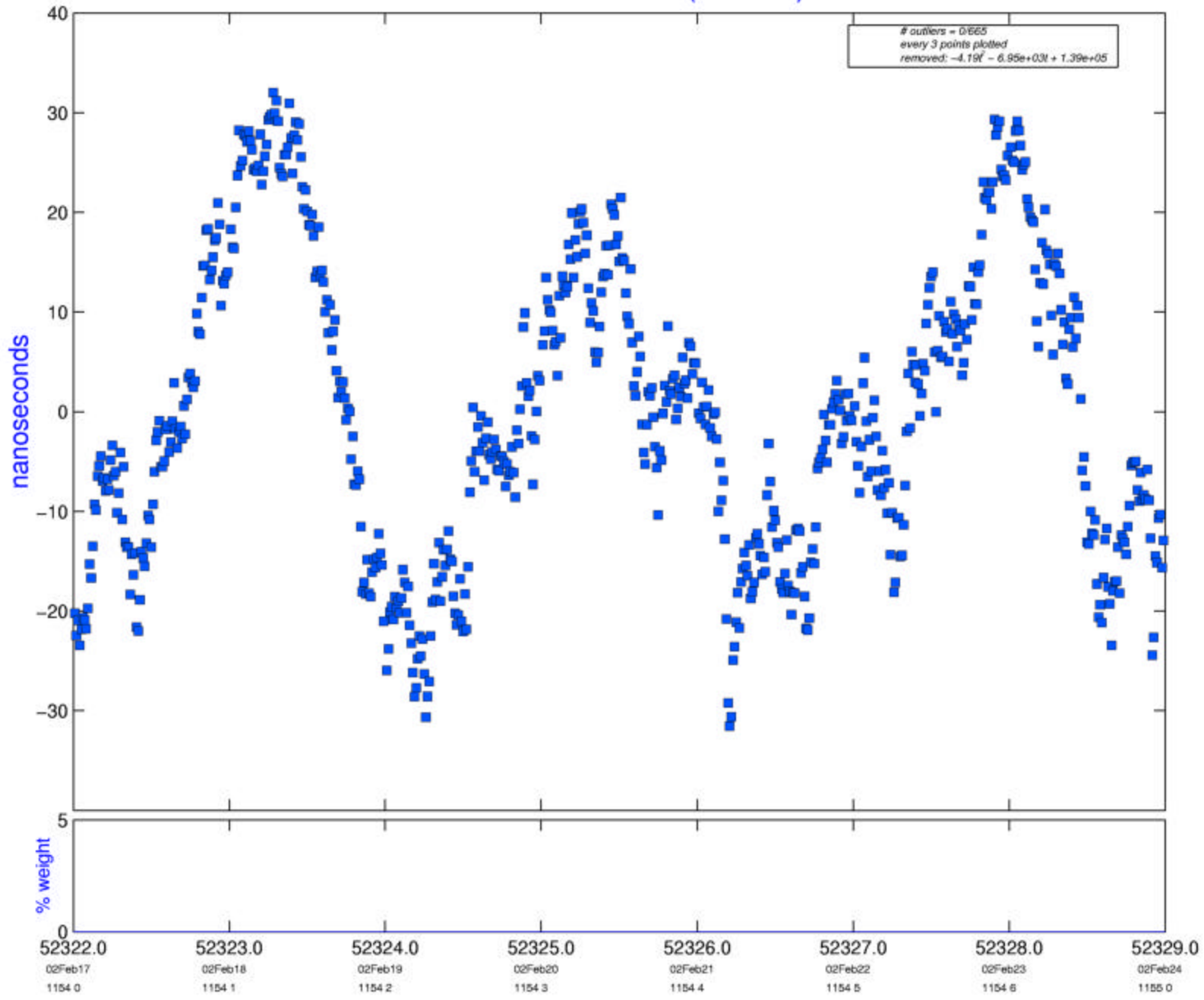
PENC w.r.t. IGRT (steered)
outliers = 0/665
every 3 points plotted
removed: −4.19t² − 6.95e+03t + 1.39e+05
nanoseconds
40
30
20
10
0
−10
−20
−30
% weight
5
0
52322.0
02Feb17
1154 0
52323.0
02Feb18
1154 1
52324.0
02Feb19
1154 2
52325.0
02Feb20
1154 3
52326.0
02Feb21
1154 4
52327.0
02Feb22
1154 5
52328.0
02Feb23
1154 6
52329.0
02Feb24
1155 0

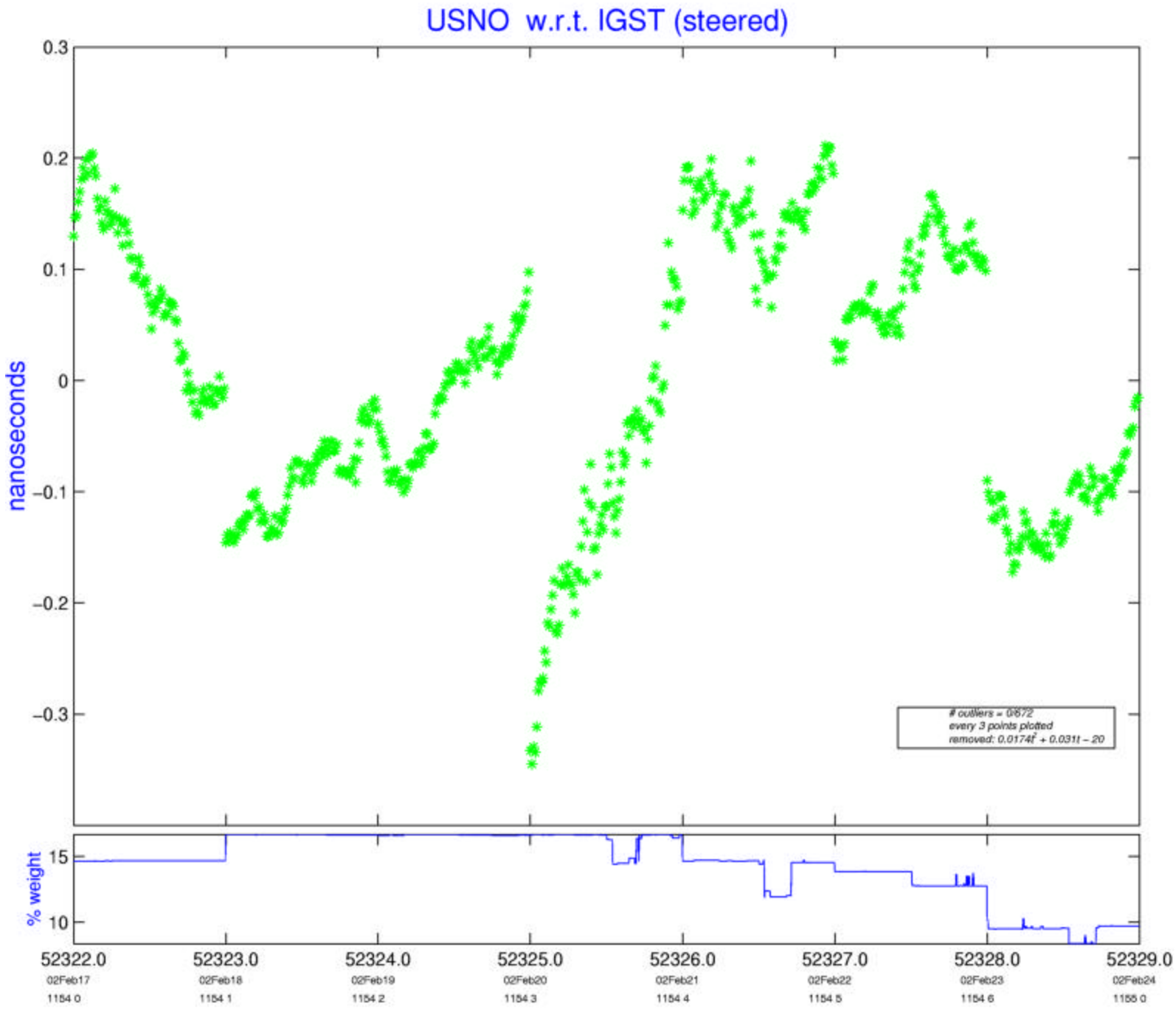
USNO w.r.t. IGST (steered)
nanoseconds
0.3
0.2
0.1
0
−0.1
−0.2
−0.3
outliers = 0672
every 3 points plotted
removed: 0.0174t² + 0.031t − 20
% weight
15
10
52322.0
52323.0
52324.0
52325.0
52326.0
52327.0
52328.0
52329.0
02Feb17
02Feb18
02Feb19
02Feb20
02Feb21
02Feb22
02Feb23
02Feb24
1154 0
1154 1
1154 2
1154 3
1154 4
1154 5
1154 6
1155 0

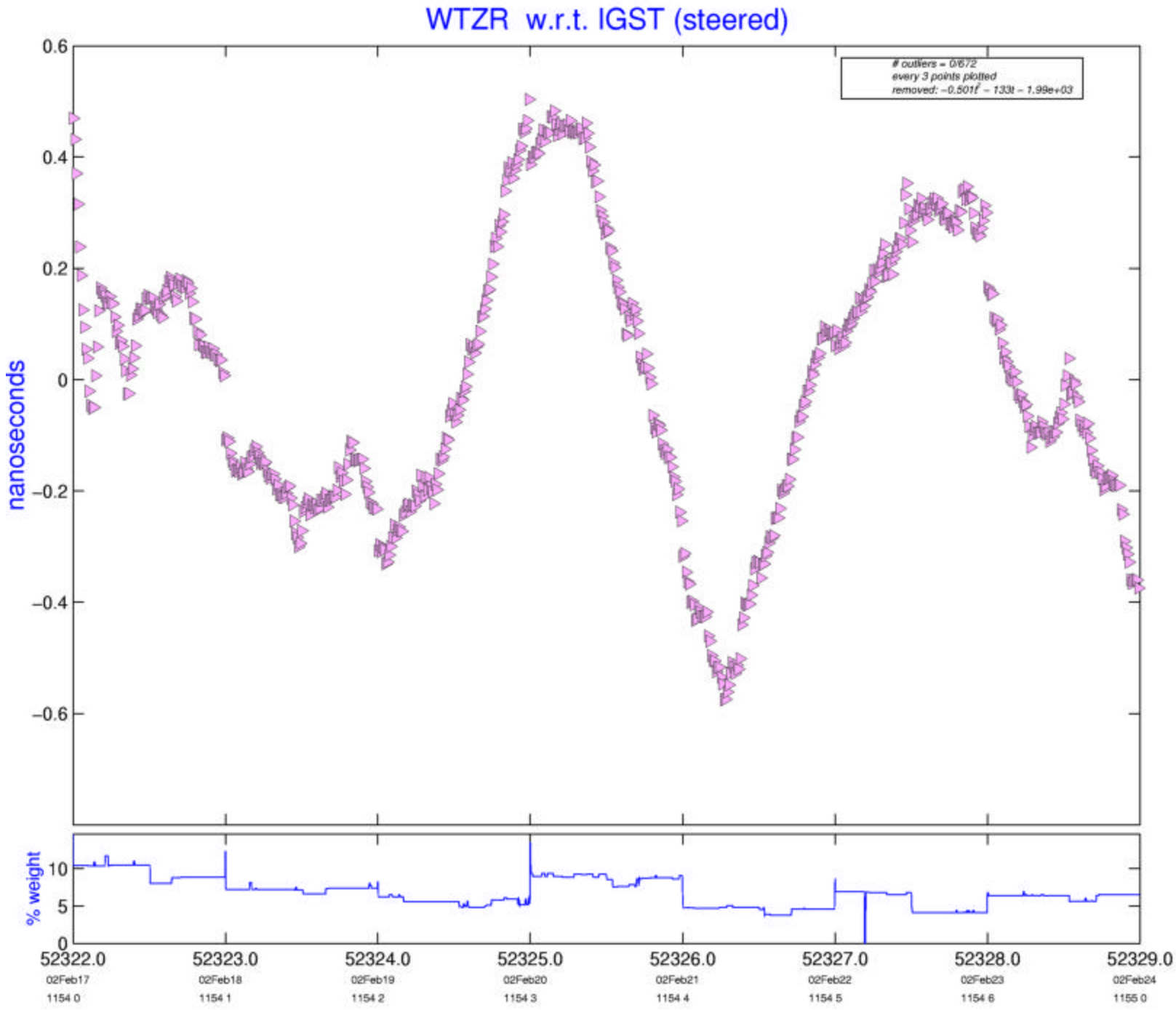
WTZR w.r.t. IGST (steered)
outliers = 0/672
every 3 points plotted
removed: −0.501t² − 133t − 1.99e+03
nanoseconds
0.6
0.4
0.2
0
−0.2
−0.4
−0.6
% weight
10
5
0
52322.0
52323.0
52324.0
52325.0
52326.0
52327.0
52328.0
52329.0
02Feb17
1154 0
02Feb18
1154 1
02Feb19
1154 2
02Feb20
1154 3
02Feb21
1154 4
02Feb22
1154 5
02Feb23
1154 6
02Feb24
1155 0

Extending the Standard Product 3 (SP3) Orbit Format

Steve Hilla
National Geodetic Survey, NOAA
1315 East-West Hwy, Silver Spring, Maryland 20910
email: steve.hilla@noaa.gov

Introduction

At the last IGS Analysis Center Workshop at USNO, it was suggested that a new SP4 orbit format be developed so that orbit files distributed by the IGS could include some type of clock accuracy information, and so that separate accuracy codes would be available for the observed versus predicted parts of the Ultra-rapid orbit files. Since modifications for adding these accuracy codes are relatively minor, they could be made in such a way as to be mostly backwards compatible; in which case the new format could be considered version C of the current SP3 format (SP3-c).

Previously, W. Gurtner and M. Rothacher have defined an SP3-b format for combined GPS/GLONASS orbits (see IGEX Mail 0042, 27-Oct-1998). This format is backwards compatible with the original Standard Product 3 format (SP3-a), with the exception of the satellite ID labels which were changed from an I3 field to a A1,I2 field to accommodate both GPS and GLONASS identifiers in a manner similar to RINEX files. Also, the orbit group at the National Imagery and Mapping Agency (NIMA) has added an "E" flag in column 75 of the SP3 Position and Clock Record, to denote a clock event (for instance, when a clock swap occurs on a satellite). The IGS can easily utilize both of these previous modifications for the new format. It has also been suggested to add "orbit event" flags as well: to denote when a satellite is in eclipse, when a portion of an orbit is predicted rather than observed, and/or when a satellite is undergoing some specific type of maneuver or change in status.

Issues/questions to consider:

*** Clock event flag** -- The clock event flag in column 75 was added by NIMA to denote epochs where their filter/smoother software re-started estimation of the clock correction because of a clock event (such as a clock swap on a satellite). For NIMA orbits, currently this field is either blank or 'E'. Should different types of clock events be represented (i.e., for GPS, GLONASS, Galileo, LEOs)? How many characters should be used? Should these flags be mandatory or optional for the ACs?

*** Orbit event flags** -- It has been suggested to also add orbit event flags to the Position and Clock Record. Such flags could use different letters to represent different types of orbit events (e.g., E = a miscellaneous orbit event, P = predicted satellite position, M = maneuver, B = boost, T = midnight turn, etc.). Or, columns 77 through 80 could be used to hold three types of flags: EPCC, where E is an eclipse flag (either E or blank), P is a predicted position/clock correction flag (either P or blank), and CC is an orbit event flag (MV = maneuver, MT = midnight turn, MD

= momentum dump, blanks, etc.). What orbit events should be represented? How might such flags prove useful to customers who use IGS orbits, or to the IGS itself? How many characters should be used? (No more than five in columns 76 through 80). Should these orbit event flags be mandatory or optional for the ACs?

*** Accuracy codes** – Since the accuracy of the predicted part of an ultra-rapid file will degrade over time, it seems preferable to have accuracy codes for each satellite at each epoch. Fortunately, the original SP3-a format used only columns 1 through 60 on each line. If the new accuracy codes are placed in columns 61 through 80, then the new format will be mostly backwards compatible with SP3-a. Listed below are four example formats which illustrate how these accuracy codes might be added. The first two examples are NOT backwards compatible: Proposal A is a very straightforward way of adding new lines for the accuracy codes using the same sized fields as before, and Proposal B uses new lines with shorter accuracy codes but adds correlation coefficients for xy, xz, xc, yz, yc, and zc (these coefficients would assist in computing user range errors). The last two examples are mostly backwards compatible since they do not add any new record types. Proposal C adds standard deviations on each line in columns 61 through 74 using the same 2**nn convention used in the SP3-a header. Proposal D adds the standard deviations using a new convention of 1.25**nn and 1.025**nn, which allows for better resolution for the standard deviations.

```
PROPOSAL A -  (EP) Satellite Position/Clock Correction standard
----------    deviations (stddevs) after each position record.
              (EV) Satellite Velocity/Rate-of-Change of Clock Corr.
              std. deviations (stddevs) after each velocity record.
              This format allows for X,Y,Z stddevs for position and
              velocity in the same units as the P and V records.
              This example includes a clock event flag in column 75
              and a two-character orbit event flag in columns 79-80.
              **Not backwards compatible since older software would
              not expect the new EP and EV records after each of
              the position and velocity records.


#cV2001  8  8  0  0  0.00000000     192 ORBIT IGS97 HLM  IGS
## 1126 259200.00000000   900.00000000 52129 0.0000000000000
+   26   G01G02G03G04G05G06G07G08G09G10G11G13G14G17G18G20G21
+        G23G24G25G26G27G28G29G30G31  0  0  0  0  0  0  0  0
+          0  0  0  0  0  0  0  0  0  0  0  0  0  0  0  0  0
+          0  0  0  0  0  0  0  0  0  0  0  0  0  0  0  0  0
+          0  0  0  0  0  0  0  0  0  0  0  0  0  0  0  0  0
++         7  8  7  8  6  7  7  7  7  7  7  7  8  8  7  9
++         9  8  6  8  7  7  6  7  7  0  0  0  0  0  0  0  0
++         0  0  0  0  0  0  0  0  0  0  0  0  0  0  0  0  0
++         0  0  0  0  0  0  0  0  0  0  0  0  0  0  0  0  0
++         0  0  0  0  0  0  0  0  0  0  0  0  0  0  0  0  0
%c G  cc GPS ccc cccc cccc cccc cccc ccccc ccccc ccccc ccccc
%c cc cc ccc ccc cccc cccc cccc cccc ccccc ccccc ccccc ccccc
%f  0.0000000  0.000000000  0.00000000000  0.000000000000000
%f  0.0000000  0.000000000  0.00000000000  0.000000000000000
%i    0    0    0    0      0      0      0      0         0
%i    0    0    0    0      0      0      0      0         0
/* ULTRA ORBIT COMBINATION FROM WEIGHTED AVERAGE OF:
/* cou esu gfu jpu siu usu
/* REFERENCED TO cou CLOCK AND TO WEIGHTED MEAN POLE:
/* CLK ANT Z-OFFSET (M): II/IIA 1.023; IIR 0.000
*  2001  8  8  0  0  0.00000000
PG01 -11044.805800 -10475.672350  21929.418200    189.163300
EP        0.000055      0.000055      0.000055      0.000222
VG01  20298.880364 -18462.044804   1381.387685     -4.534317
EV        0.000022      0.000022      0.000022      0.000111
PG02 -12593.593500  10170.327650 -20354.534400    -55.976000                  MD
EP        0.000055      0.000055      0.000055      0.000222
VG02  -9481.923808 -25832.652567  -7277.160056      8.801258
EV        0.000022      0.000022      0.000022      0.000111
PG03   9335.606450 -21952.990750 -11624.350150     54.756700
```

```
EP        0.000055      0.000055      0.000055      0.000222
VG03  12497.392894  -8482.260298  26230.348459      5.620682
EV        0.000022      0.000022      0.000022      0.000111
PG04 -16148.976900   8606.630600  19407.845050    617.997800
EP        0.000055      0.000055      0.000055      0.000222
VG04 -22859.768469  -8524.538983 -15063.229095     -3.292980
EV        0.000022      0.000022      0.000022      0.000111
PG05  13454.631450  20956.333700   9376.994100    308.956400
EP        0.000055      0.000055      0.000055      0.000222
VG05    392.255680  12367.086937 -27955.768747    -13.600595
EV        0.000022      0.000022      0.000022      0.000111
PG06  18821.523100   1138.155450  18958.305500     -2.406900
EP        0.000055      0.000055      0.000055      0.000222
VG06 -16239.818866  17326.208695  15006.894015     12.496639
EV        0.000022      0.000022      0.000022      0.000111
PG07 -20393.814200  16198.067550  -4138.151700    428.892900
EP        0.000055      0.000055      0.000055      0.000222
VG07   1578.105130  -6536.248480 -30974.730074      2.828360
EV        0.000022      0.000022      0.000022      0.000111
PG08 -23592.378250   1395.049800 -12524.037100    461.972900
EP        0.000055      0.000055      0.000055      0.000222
VG08 -13996.847785  -6945.665482  25908.199568      0.364488
EV        0.000022      0.000022      0.000022      0.000111
PG09  17353.533200  15151.105700 -13851.534050     -1.841700
EP        0.000055      0.000055      0.000055      0.000222
VG09 -16984.306646  -2424.913336 -23969.277677    -14.371692
EV        0.000022      0.000022      0.000022      0.000111
PG10    947.048150  25410.786050   7257.797800      8.238800              E
EP        0.000055      0.000055      0.000055      0.000222
VG10  -4368.825926  -8497.316296  30474.278851     13.823775
EV        0.000022      0.000022      0.000022      0.000111
  .
  .
  .
```

PROPOSAL B - (EP) Satellite Position/Clock Correction stddevs, and correlation coefficients, after each position record. (EV) Satellite Velocity/Rate-of-Change of Clock Correction standard deviations (stddevs), and correlation coefficients, after each velocity record. This example includes a clock event flag in column 75 and a two-character orbit event flag in columns 79-80. **Not backwards compatible since older software would not expect the new EP and EV records after each of the position and velocity records.

This format is similar to Proposal A but also includes correlation information for the position and velocity records. Columns 1 through 26 would use: EPbbxxxxbyyyybzzzzbccccccc, where b is a reserved blank space, xxxx is the X-coord/X-veloc. stddev in mm or 10**-4 mm/sec, yyyy is the Y-coord/Y-veloc. stddev in mm or 10**-4 mm/sec, zzzz is the Z-coord/Z-veloc. stddev in mm or 10**-4 mm/sec, ccccccc is the clock/clock-rate stddev in psec or 10**-4 psec/sec. Columns 27 through 80 then use 6(1x,i8) to store the correlation coefficients for xy, xz, xc, yz, yc, zc. Each 7-digit integer would be divided by 10,000,000 to produce a correlation coefficient between -0.9999999 and +0.9999999.

```
#cV2001  8  8  0  0  0.00000000     192 ORBIT IGS97 HLM  IGS
## 1126 259200.00000000   900.00000000 52129 0.0000000000000
+   26   G01G02G03G04G05G06G07G08G09G10G11G13G14G17G18G20G21
+        G23G24G25G26G27G28G29G30G31  0  0  0  0  0  0  0  0
+          0  0  0  0  0  0  0  0  0  0  0  0  0  0  0  0  0
+          0  0  0  0  0  0  0  0  0  0  0  0  0  0  0  0  0
+          0  0  0  0  0  0  0  0  0  0  0  0  0  0  0  0  0
++         7  8  7  8  6  7  7  7  7  7  7  7  8  8  7  9
++         9  8  6  8  7  7  6  7  7  0  0  0  0  0  0  0  0
++         0  0  0  0  0  0  0  0  0  0  0  0  0  0  0  0  0
++         0  0  0  0  0  0  0  0  0  0  0  0  0  0  0  0  0
++         0  0  0  0  0  0  0  0  0  0  0  0  0  0  0  0  0
%c G  cc GPS ccc cccc cccc cccc cccc ccccc ccccc ccccc ccccc
%c cc cc ccc ccc cccc cccc cccc cccc ccccc ccccc ccccc ccccc
%f  0.0000000  0.000000000  0.00000000000  0.000000000000000
%f  0.0000000  0.000000000  0.00000000000  0.000000000000000
%i    0    0    0    0      0      0      0      0         0
%i    0    0    0    0      0      0      0      0         0
/* ULTRA ORBIT COMBINATION FROM WEIGHTED AVERAGE OF:
```

```
/* cou esu gfu jpu siu usu
/* REFERENCED TO cou CLOCK AND TO WEIGHTED MEAN POLE:
/* CLK ANT Z-OFFSET (M): II/IIA 1.023; IIR 0.000
*  2001  8  8  0  0  0.00000000
PG01 -11044.805800 -10475.672350  21929.418200    189.163300                   MD
EP    55   55   55     222  1234567 -1234567  9999999 -9999999  9990000 -9990000
VG01  20298.880364 -18462.044804   1381.387685     -4.534317
EV    22   22   22     111  1234567 -1234567  9999999 -9999999  9990000 -9990000
PG02 -12593.593500  10170.327650 -20354.534400    -55.976000
EP    55   55   55     222  1234567 -1234567  9999999 -9999999  9990000 -9990000
VG02  -9481.923808 -25832.652567  -7277.160056      8.801258
EV    22   22   22     111  1234567 -1234567  9999999 -9999999  9990000 -9990000
PG03   9335.606450 -21952.990750 -11624.350150     54.756700
EP    55   55   55     222  1234567 -1234567  9999999 -9999999  9990000 -9990000
VG03  12497.392894  -8482.260298  26230.348459      5.620682
EV    22   22   22     111  1234567 -1234567  9999999 -9999999  9990000 -9990000
PG04 -16148.976900   8606.630600  19407.845050    617.997800
EP    55   55   55     222  1234567 -1234567  9999999 -9999999  9990000 -9990000
VG04 -22859.768469  -8524.538983 -15063.229095     -3.292980
EV    22   22   22     111  1234567 -1234567  9999999 -9999999  9990000 -9990000
PG05  13454.631450  20956.333700   9376.994100    308.956400
EP    55   55   55     222  1234567 -1234567  9999999 -9999999  9990000 -9990000
VG05    392.255680  12367.086937 -27955.768747    -13.600595
EV    22   22   22     111  1234567 -1234567  9999999 -9999999  9990000 -9990000
PG06  18821.523100   1138.155450  18958.305500     -2.406900
EP    55   55   55     222  1234567 -1234567  9999999 -9999999  9990000 -9990000
VG06 -16239.818866  17326.208695  15006.894015     12.496639
EV    22   22   22     111  1234567 -1234567  9999999 -9999999  9990000 -9990000
PG07 -20393.814200  16198.067550  -4138.151700    428.892900
EP    55   55   55     222  1234567 -1234567  9999999 -9999999  9990000 -9990000
VG07   1578.105130  -6536.248480 -30974.730074      2.828360
EV    22   22   22     111  1234567 -1234567  9999999 -9999999  9990000 -9990000
PG08 -23592.378250   1395.049800 -12524.037100    461.972900
EP    55   55   55     222  1234567 -1234567  9999999 -9999999  9990000 -9990000
VG08 -13996.847785  -6945.665482  25908.199568      0.364488
EV    22   22   22     111  1234567 -1234567  9999999 -9999999  9990000 -9990000
PG09  17353.533200  15151.105700 -13851.534050     -1.841700
EP    55   55   55     222  1234567 -1234567  9999999 -9999999  9990000 -9990000
VG09 -16984.306646  -2424.913336 -23969.277677    -14.371692
EV    22   22   22     111  1234567 -1234567  9999999 -9999999  9990000 -9990000
PG10    947.048150  25410.786050   7257.797800      8.238800                    E
EP    55   55   55     222  1234567 -1234567  9999999 -9999999  9990000 -9990000
VG10  -4368.825926  -8497.316296  30474.278851     13.823775
 .
 .
 .



PROPOSAL C -  Satellite Position/Clock Correction stddevs on each
----------    position record (in columns 61 through 74).
              Satellite Velocity/Rate-of-Change of Clock Correction
              standard deviations (stddevs) on each
              velocity record (in columns 61 through 74).
              This format includes X,Y,Z stddevs for position & velocity,
              a clock event flag, and a two-character orbit event flag.
              ** this format should be mostly backwards compatible since
              most current software does not use columns 61 through 74.

       The main question here is how to handle columns 61 through 74.
       The example below uses: bxxbyybzzbccbbEbbbMM, where
       b is a reserved blank space,
       xx is the X-coord/X-veloc. stddev in 2**n mm or 10**-4 mm/sec,
       yy is the Y-coord/Y-veloc. stddev in 2**n mm or 10**-4 mm/sec,
       zz is the Z-coord/Z-veloc. stddev in 2**n mm or 10**-4 mm/sec,
       cc is the clock/clock-rate stddev in 2**n psec or 10**-4 psec/sec.

       E  is a clock event flag
       MM is an orbit event flag


#cV2001  8  8  0  0  0.00000000     192 ORBIT IGS97 HLM  IGS
## 1126 259200.00000000   900.00000000 52129 0.0000000000000
+   26   G01G02G03G04G05G06G07G08G09G10G11G13G14G17G18G20G21
+        G23G24G25G26G27G28G29G30G31  0  0  0  0  0  0  0  0
+          0  0  0  0  0  0  0  0  0  0  0  0  0  0  0  0  0
+          0  0  0  0  0  0  0  0  0  0  0  0  0  0  0  0  0
+          0  0  0  0  0  0  0  0  0  0  0  0  0  0  0  0  0
++         7  8  7  8  6  7  7  7  7  7  7  7  7  8  8  7  9
++         9  8  6  8  7  7  6  7  7  0  0  0  0  0  0  0  0
```

```
++         0  0  0  0  0  0  0  0  0  0  0  0  0  0  0  0  0
++         0  0  0  0  0  0  0  0  0  0  0  0  0  0  0  0  0
++         0  0  0  0  0  0  0  0  0  0  0  0  0  0  0  0  0
%c G  cc GPS ccc cccc cccc cccc cccc ccccc ccccc ccccc ccccc
%c cc cc ccc ccc cccc cccc cccc cccc ccccc ccccc ccccc ccccc
%f  0.0000000  0.000000000  0.00000000000  0.000000000000000
%f  0.0000000  0.000000000  0.00000000000  0.000000000000000
%i    0    0    0    0      0      0      0      0         0
%i    0    0    0    0      0      0      0      0         0
/* ULTRA ORBIT COMBINATION FROM WEIGHTED AVERAGE OF:
/* cou esu gfu jpu siu usu
/* REFERENCED TO cou CLOCK AND TO WEIGHTED MEAN POLE:
/* CLK ANT Z-OFFSET (M): II/IIA 1.023; IIR 0.000
*  2001  8  8  0  0  0.00000000
PG01 -11044.805800 -10475.672350  21929.418200    189.163300  6  6  6  8
VG01  20298.880364 -18462.044804   1381.387685     -4.534317  4  4  4  7
PG02 -12593.593500  10170.327650 -20354.534400    -55.976000  6  6  6  8       MD
VG02  -9481.923808 -25832.652567  -7277.160056      8.801258  4  4  4  7
PG03   9335.606450 -21952.990750 -11624.350150     54.756700  6  6  6  8
VG03  12497.392894  -8482.260298  26230.348459      5.620682  4  4  4  7
PG04 -16148.976900   8606.630600  19407.845050    617.997800  6  6  6  8
VG04 -22859.768469  -8524.538983 -15063.229095     -3.292980  4  4  4  7
PG05  13454.631450  20956.333700   9376.994100    308.956400  6  6  6  8
VG05    392.255680  12367.086937 -27955.768747    -13.600595  4  4  4  7
PG06  18821.523100   1138.155450  18958.305500     -2.406900  6  6  6  8
VG06 -16239.818866  17326.208695  15006.894015     12.496639  4  4  4  7
PG07 -20393.814200  16198.067550  -4138.151700    428.892900  6  6  6  8
VG07   1578.105130  -6536.248480 -30974.730074      2.828360  4  4  4  7
PG08 -23592.378250   1395.049800 -12524.037100    461.972900  6  6  6  8
VG08 -13996.847785  -6945.665482  25908.199568      0.364488  4  4  4  7
PG09  17353.533200  15151.105700 -13851.534050     -1.841700  6  6  6  8
VG09 -16984.306646  -2424.913336 -23969.277677    -14.371692  4  4  4  7
PG10    947.048150  25410.786050   7257.797800      8.238800  6  6  6  8  E
VG10  -4368.825926  -8497.316296  30474.278851     13.823775  4  4  4  7
 .
 .
 .
```

PROPOSAL D - Satellite Position/Clock Correction stddevs on each position record (in columns 61 through 74). Satellite Velocity/Rate-of-Change of Clock Correction standard deviations (stddevs) on each velocity record (in columns 61 through 74). This format includes X,Y,Z stddevs for position & velocity, a clock event flag, and a two-character orbit event flag. ** this format should be mostly backwards compatible since most software currently does not use columns 61 through 74.

Again, the question here is how to handle columns 61 through 74. This proposal differs from C only by columns 62 through 73. The example below uses: bxxbyybzzbcccbEbbbMM, where b is a reserved blank space,
xx is the X-coord/X-veloc. stddev in 1.25**nn mm or 10**-4 mm/sec,

yy is the Y-coord/Y-veloc. stddev in 1.25**nn mm or 10**-4 mm/sec,

zz is the Z-coord/Z-veloc. stddev in 1.25**nn mm or 10**-4 mm/sec,

ccc is the clock/clock-rate stddev in 1.025**nnn psec or 10**-4 psec/sec.
E is a clock event flag
MM is an orbit event flag

Note: This format has been suggested by Ben Remondi. His idea for using a floating point base**exponent approach, rather than 2**nn, has considerably better resolution than Proposal C. For example, if one is trying to represent a position stddev of 55 mm, the closest 2**nn value is 64. Using 1.25**18 gives a value of 55.51. Similarly, if one has a Clock Corr stddev of 198 picoseconds, the closest 2**nn value is 256. Using 1.025**214 gives a value of 197.20. Using 2**nn seems somewhat wasteful since the higher exponents would never be used (e.g., 2**60 = 1.15 * 10**18 and 2**98 = 3.17 * 10**29). The exponent 0 would represent 1.0 units. Stddev information would not be required; in cases where the stddevs were unknown, the stddev columns would be blank. The exponents 99 and 999 can be reserved, they would mean that the stddev was too large to compute (which is unlikely since 1.25**98 is 3,141,819,817.8 and 1.025**998 is 50,398,505,821.8). The suggested base numbers, 1.25 and 1.025, could possibly be modified to handle a smaller range, but once chosen, they would remain fixed (i.e., two base numbers would be defined in the new orbit

```
format, one for the pos/vel stddevs and one for the clock correction/rate-
of-change of clock correction stddevs).


#cV2001  8  8  0  0  0.00000000     192 ORBIT IGS97 HLM  IGS
## 1126 259200.00000000   900.00000000 52129 0.0000000000000
+   26   G01G02G03G04G05G06G07G08G09G10G11G13G14G17G18G20G21
+        G23G24G25G26G27G28G29G30G31  0  0  0  0  0  0  0  0
+          0  0  0  0  0  0  0  0  0  0  0  0  0  0  0  0  0
+          0  0  0  0  0  0  0  0  0  0  0  0  0  0  0  0  0
+          0  0  0  0  0  0  0  0  0  0  0  0  0  0  0  0  0
++         7  8  7  8  6  7  7  7  7  7  7  7  8  8  7  9
++         9  8  6  8  7  7  6  7  7  0  0  0  0  0  0  0  0
++         0  0  0  0  0  0  0  0  0  0  0  0  0  0  0  0  0
++         0  0  0  0  0  0  0  0  0  0  0  0  0  0  0  0  0
++         0  0  0  0  0  0  0  0  0  0  0  0  0  0  0  0  0
%c G  cc GPS ccc cccc cccc cccc cccc cccc ccccc ccccc ccccc ccccc
%c cc cc ccc ccc cccc cccc cccc cccc cccc ccccc ccccc ccccc ccccc
%f  0.0000000  0.000000000  0.00000000000  0.000000000000000
%f  0.0000000  0.000000000  0.00000000000  0.000000000000000
%i    0    0    0    0      0      0      0      0         0
%i    0    0    0    0      0      0      0      0         0
/* ULTRA ORBIT COMBINATION FROM WEIGHTED AVERAGE OF:
/* cou esu gfu jpu siu usu
/* REFERENCED TO cou CLOCK AND TO WEIGHTED MEAN POLE:
/* CLK ANT Z-OFFSET (M): II/IIA 1.023; IIR 0.000
*  2001  8  8  0  0  0.00000000
PG01 -11044.805800 -10475.672350  21929.418200    189.163300 18 18 18 219
VG01  20298.880364 -18462.044804   1381.387685     -4.534317 14 14 14 191
PG02 -12593.593500  10170.327650 -20354.534400    -55.976000 18 18 18 219     MD
VG02  -9481.923808 -25832.652567  -7277.160056      8.801258 14 14 14 191
PG03   9335.606450 -21952.990750 -11624.350150     54.756700 18 18 18 219
VG03  12497.392894  -8482.260298  26230.348459      5.620682 14 14 14 191
PG04 -16148.976900   8606.630600  19407.845050    617.997800 18 18 18 219
VG04 -22859.768469  -8524.538983 -15063.229095     -3.292980 14 14 14 191
PG05  13454.631450  20956.333700   9376.994100    308.956400 18 18 18 219
VG05    392.255680  12367.086937 -27955.768747    -13.600595 14 14 14 191
PG06  18821.523100   1138.155450  18958.305500     -2.406900 18 18 18 219
VG06 -16239.818866  17326.208695  15006.894015     12.496639 14 14 14 191
PG07 -20393.814200  16198.067550  -4138.151700    428.892900 18 18 18 219
VG07   1578.105130  -6536.248480 -30974.730074      2.828360 14 14 14 191
PG08 -23592.378250   1395.049800 -12524.037100    461.972900 18 18 18 219
VG08 -13996.847785  -6945.665482  25908.199568      0.364488 14 14 14 191
PG09  17353.533200  15151.105700 -13851.534050     -1.841700 18 18 18 219
VG09 -16984.306646  -2424.913336 -23969.277677    -14.371692 14 14 14 191
PG10    947.048150  25410.786050   7257.797800      8.238800 18 18 18 219 E
VG10  -4368.825926  -8497.316296  30474.278851     13.823775 14 14 14 191
 .
 .
 .
```

*** Recommendations** -- It is recommended that the IGS adopt Proposal D. The main problem with Proposals A and B is that, while they are easier to read or might offer additional data, they would increase the size of the orbit files significantly and they are not backwards compatible. Proposals C and D are almost identical. Although the accuracy codes in Proposal D use a numerical convention that is quite different than that used in the header, the added resolution it provides is probably worth the risk of any possible confusion (hopefully, most persons seeing an SP3-c file for the first time will consult the new format specification and not just assume that the new accuracy codes still use 2**n). At the Ottawa workshop, it remains to be decided what types of orbit event flags, if any, should be defined for SP3-c.

A few important points need to be stressed regarding backwards compatibility. There are two small but significant changes being proposed for SP3-c 1.) Like SP3-b, the satellite ID label is being changed from an I3 field (PRN 2 is " 2") to an A1,I2 field (PRN 2 is "G02"). This will require modifying all older C and Fortran programs which can now read only the SP3-a format. 2.) More columns are being added to each line, thus going from a 60-column file to an 80-column

file. This will be no problem for most Fortran programs, but will require modifying some older C and C++ programs (if they happen to use fgets(), getline(), etc., with a character array that is dimensioned with less than 80 characters). To accommodate users with older software, the IGS will be required to store both SP3-a files and SP3-c files on its website (at least until most software has been updated to read the new format). The IGS may want to announce some interim period for providing both types of files (one year ?), after which, it would make conversion software available to those users still needing SP3-a files.

Acknowledgements
The author would like to thank several people who provided comments and suggestions regarding these proposed formats: Werner Gurtner, Jan Kouba, Stephen Malys, Tomas Martin Mur, Jim Ray, Benjamin Remondi, Markus Rothacher, Mark Schenewerk, Everett Swift, and Robert Weber.

References

Remondi, B.W., 1989, Extending the National Geodetic Survey Standard GPS Orbit Formats, NOAA Technical Report NOS 133 NGS 46, 85 pp.

Remondi, B.W., 1991, NGS Second Generation ASCII and Binary Orbit Formats and Associated Interpolation Studies, presented at the Twentieth General Assembly of the International Union of Geodesy and Geophysics, Vienna, Austria, August 11-24.

The original SP3-a format specification can be viewed at
http://igscb.jpl.nasa.gov/igscb/data/format/sp3_docu.txt

The NIMA SP3 format can be viewed at
http://164.214.2.59/GandG/sathtml/sp3format.html

The IGEX98 SP3-b format can be viewed at
http://igscb.jpl.nasa.gov/mail/igexmail/1998/msg00041.html